sustainability

MDPI

Review

A Review of the Use of Hydrogen in Compression Ignition Engines with Dual-Fuel Technology and Techniques for Reducing NO_x Emissions

Juan Manuel Rueda-Vázquez [1], Javier Serrano [2], Sara Pinzi [1], Francisco José Jiménez-Espadafor [2] and M. P. Dorado [1,*]

[1] Department of Physical Chemistry and Applied Thermodynamics, Universidad de Córdoba, Edificio Leonardo da Vinci, Campus de Rabanales, Campus de Excelencia Internacional Agroalimentario ceiA3, 14071 Cordoba, Spain; jmrueda@uco.es (J.M.R.-V.); qf1pinps@uco.es (S.P.)

[2] Department of Energy Engineering, Universidad de Sevilla, Spain, Camino de los Descubrimientos, s/n, 41092 Sevilla, Spain; jserrano9@us.es (J.S.); fcojjea@us.es (F.J.J.-E.)

* Correspondence: pilar.dorado@uco.es; Tel.: +34-957-21-83-32

Abstract: The use of compression ignition engines (CIEs) is associated with increased greenhouse gas emissions. It is therefore necessary to research sustainable solutions and reduce the negative environmental impact of these engines. A widely studied alternative is the use of H_2 in dual-fuel mode. This review has been developed to include the most recent studies on the subject to collect and compare their main conclusions on performance and emissions. Moreover, this study includes most relevant emission control strategies that have not been extensively analyzed in other reviews on the subject. The main conclusion drawn from the literature is the negative effect of the addition of H_2 on NO_x. This is due to the increase in temperature during combustion, which increases NO_x formation, as the thermal mechanism predominates. Therefore, to reduce these emissions, three strategies have been studied, namely exhaust gas recirculation (EGR), water injection (WI), and compression ratio (CR) reduction. The effect of these techniques on NO_x reduction, together with their effect on other analyzed performance parameters, have been deeply analyzed. The studies reviewed in this work indicate that hydrogen is an alternative fuel for CIEs when used in conjunction with techniques that have proven to be effective in reducing NO_x.

Keywords: sustainable fuel; exhaust gas recirculation; water injection; compression rate; diesel engine; hydrogen energy share

Citation: Rueda-Vázquez, J.M.; Serrano, J.; Pinzi, S.; Jiménez-Espadafor, F.J.; Dorado, M.P. A Review of the Use of Hydrogen in Compression Ignition Engines with Dual-Fuel Technology and Techniques for Reducing NO_x Emissions. *Sustainability* **2024**, *16*, 3462. https://doi.org/10.3390/su16083462

Academic Editor: Brantley T. Liddle

Received: 15 March 2024
Revised: 8 April 2024
Accepted: 18 April 2024
Published: 21 April 2024

1. Introduction

The global demand for energy is increasing annually, mainly due to the growth of the world's population. This is directly related to the use of fossil fuels, which have become the primary source of energy in certain sectors, such as power generation, transportation, heating, industry, and building. The use of these fuels is directly linked to the emission of CO_2, one of the main greenhouse gases (GHGs). According to the European Commission's report on global GHG emissions [1], in 2022, CO_2 emissions were more than twice as high as in 1970 (53.8 Gt vs. 25 Gt). In that year, CO_2 emissions reached their highest annual average concentration in the atmosphere at 417 ppm, which was about 50% higher than at the beginning of the Industrial Revolution in 1760 (280 ppm) [2,3].

To reduce these emissions into the atmosphere and their contribution to global warming, governments have implemented stringent emission regulations. The Paris Agreement, signed in 2015 at COP21, sets long-term goals for countries to take action to limit the global temperature increase to 2 °C above pre-industrial levels. It also includes working with developing countries to mitigate climate change [4]. However, both COP26 and COP27 concluded to set this limit at 1.5 °C. In addition, the European climate legislation (called "Fit

for 55") is part of the European Green Deal, which aims to reduce its net GHG emissions by at least 55% by 2030 compared to 1990 levels and to become carbon neutral by 2050 [5]. These measures have a major impact on the transport sector, which is responsible for GHG emissions as well as other pollutants, such as CO, NO_x, unburned hydrocarbons (HC), and particulate matter (PM). The European Commission has imposed stricter CO_2 emission targets for 2020 for this sector. These targets are 95, 93.6, and 49.5 g CO_2/km for the periods of 2020–2024, 2025–2029, and 2030–2034, respectively. From 2035, the target is a 100% reduction, meaning carbon neutrality [6].

In this regard, extensive efforts are being made to search for different techniques to either improve the efficiency of thermal engines or alternative forms of propulsion, such as electrification. Regarding the latter, it seems that the transportation sector is moving towards electrification, according to reports by British Petroleum [7], the International Transport Forum [8], and McKinsey & Company [9]. However, thermal engines, particularly compression ignition engines (CIEs), still have a key role to play in transportation and other sectors (such as agriculture, aviation, and power generation). To improve the efficiency of thermal engines, various studies focus on two different strategies that reduce pollutants and do not require significant engine modifications [10–12].

The first is the use of biofuels to replace carbon-based fuels. For more than 25 years, to improve their performance and production, research on biofuels has been developed worldwide. The use of biofuels has several advantages, including the use of fuel properties close to those of diesel fuel, the fact that they can be used directly in CIEs without significant engine modifications, and the fact that there is no production of sulfur oxides [13]. Biodiesel is the most widely used biofuel for CIEs; the most common feedstocks are vegetable oils derived from edible plants, such as rapeseed, palm, soybean, sunflower, and other oleaginous crops [14]. However, the use of the above biofuels may be affected by global regulations (such as the European Green Deal) affecting the production and sale of first-generation biofuels (from feedstocks that may cause land use change). However, research continues into blending these fuels with other components, i.e., alcohols, as well as the development of second-generation (solid urban and agricultural waste, such as used oil, plastic, and biomass) and third-generation (algae carbohydrate) biofuels.

The second strategy is the use of a carbon-free gaseous fuel, such as hydrogen (H_2). H_2 is an energy carrier with a wide range of fuel applications, such as direct use in internal combustion engines (ICEs), heaters, or fuel cells. In addition, the adaptation of existing ICEs to this gas makes possible the transition of the transportation sector to a hydrogen-based economy. The properties of this gas are discussed in Section 2, but some of the advantages of H_2 over other fossil fuels are its zero-carbon content and high energy density in terms of mass (120 MJ/kg, about three times that of carbon-based fuels) (see Table 1). Despite its zero-carbon content, the vast majority of H_2 production, about 90 Mt in 2020, is derived from fossil fuels through steam methane reforming (SMR), partial oxidation and autothermal reforming, or steam–oxygen gasification of coal, resulting in the generation of 900 Mt of CO_2 [15,16]. However, H_2 production from renewable energy and natural sources, such as water, which can split O_2 and H_2 molecules through electrolysis, reduces CO_2 emissions to zero [17].

However, H_2 cannot be used as the sole fuel in CIEs due to its high autoignition temperature (328 K above that of diesel fuel, see Table 1). Therefore, the addition of another fuel with a lower autoignition temperature to act as a combustion activator (usually in liquid form, such as diesel fuel or biofuels) is needed. This mode of engine operation, in which two different fuels are used simultaneously, is called dual-fuel operation. Typically, H_2 is introduced into the intake manifold while diesel fuel is injected directly into the combustion chamber, although other methods can be used, as shown in Section 2. The use of H_2 provides significantly different combustion and emission characteristics.

Table 1. H_2 properties compared with natural gas, diesel fuel, and gasoline [18,19].

Property	Unit	Hydrogen (Gas)	Natural Gas	Diesel Fuel (Liquid)	Gasoline (Liquid)
Density at normal conditions	kg/m^3	0.0899	0.7–0.9	820–950	730–780
Autoignition temperature	K	858	813	530	620
Octane/cetane number		130	120	40–55	86–98
Lower heating value	MJ/kg	120	53.6	43.9	42.5
Diffusivity in air	cm^2/s	0.63	0.24	0.038	
Stoichiometric air–fuel ratio		34.2	17.2	14.5	14.7
Flammability limits	% *v*/*v* in air	4–76	5.3–15	0.6–5.5	1–7.6
Minimum energy for ignition in air	mJ	0.02	0.29		0.24
Specific heat of hydrogen gas at constant pressure (C_P)	J/kgK	14,200	2340	2050	2100

The study of H_2 as a fuel in CIEs in dual-fuel mode is a growing topic. Rueda-Vázquez et al. [20] conducted a bibliometric study and found an increase in the number of publications and citations per year on this topic in the Web of Science from 2010 to 2021. However, studies on this technology started in the 1990s. The results, updated to 2023, are shown in Figure 1.

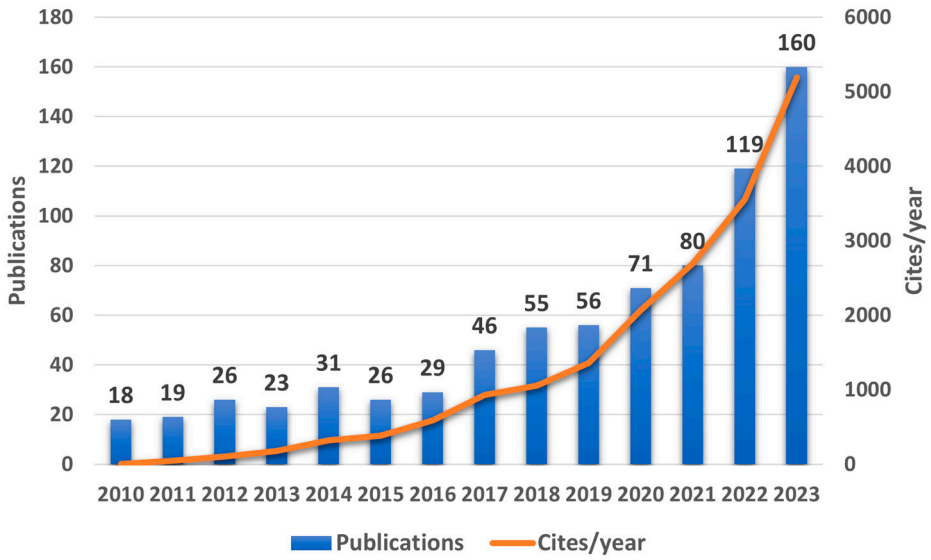

Figure 1. Number of publications and citations per year about the use of H_2 in combustion ignition engines under dual-fuel mode.

According to the literature, a main drawback of the use of H_2 as a fuel in CIEs is the generation of NO_x [21–25]. Due to higher peaks in the heat release rate (HRR) and combustion chamber temperature, NO_x emissions are increased. The Zeldovich mechanism is one of the main mechanisms that contributes to NO_x formation [23,25]. Various strategies are used to control NO_x emissions, such as exhaust gas recirculation (EGR) and water injection and either direct water injection (DWI) or water injection into the intake manifold (WI). Another strategy developed to control NO_x emissions in CIEs is the reduction of the compression ratio (CR) or the addition of NH_3 [26,27].

The aim of this review is to provide a detailed review of recent work on the addition of H_2 to CIEs. This work distinguishes between multi-cylinder engines, whose main application may be in the transport sector, and single-cylinder engines used for other purposes, i.e., agricultural machinery. The majority of the works consulted are those in which the ignition source is diesel fuel, with the exception of biofuels.

The objectives of this research are as follows:

1. To evaluate the main properties of H_2 with respect to other carbon-based fuels. It also includes advantages and disadvantages of its use in CIEs, enumerating different strategies for introducing the gas into the engine.
2. To analyze in detail the influence of the use of H_2 in a CIE in dual-fuel mode in terms of performance and emissions.
3. To evaluate different strategies to reduce the increase in NO_x emissions associated with the use of H_2.

2. Hydrogen as Fuel in Compression Ignition Engines

H_2 is the lightest gas in the periodic table of elements (14 times lighter than air). It is highly flammable and odorless, and it burns with a colorless flame [28]. It is usually found in its molecular form under normal conditions. Some of the most important properties of H_2 with respect to other carbon-based fuels are shown in Table 1.

H_2 is a carbon-free fuel, and one of its main advantages is its lower heating value (LHV). Its LHV is about double that of natural gas (NG) and triple that of diesel fuel and gasoline. However, due to its low density, a large amount of H_2 is required to produce the same amount of energy as these fuels, which can lead to a storage problem. The most common method of storing H_2 is to compress it in high-pressure vessels. H_2 vessels are mainly divided into four different types (Type I to Type IV). Type I (all metal) and Type II (metal liner with hoop wrapping) cannot be used in vehicles due to their lower H_2 storage density and serious H_2 embrittlement problems [29]. Currently, Type III (metal liner with full wrapping) and Type IV (plastic liner with full wrapping) are commonly used in fuel cell vehicles (FCV). Other vehicle-compatible and widely studied H_2 storage systems include cryogenic or cryo-compressed storage [30,31].

Also worth mentioning are its high flammability limits, making it suitable for a wide range of air–fuel mixtures and engine powers, with the advantage that H_2 can run on a lean mixture [32]. Its high diffusivity allows for reducing the heterogeneity of a diesel spray, resulting in a better and more uniform premixing with air [33]. This better mixture implies better conditions for the complete combustion process. As mentioned above, H_2 cannot work exclusively in a conventional CIE, because its high auto-ignition temperature (858 K) is significantly higher than that of other fuels, which makes ignition difficult when the temperature rises during compression stroke. Therefore, this gas must always work together with another fuel, with a lower autoignition temperature, to act as an ignition source. The amount of H_2 supplied to the engine can be indicated in two ways; directly, by specifying the amount of H_2 supplied, or indirectly, by using a parameter that relates the energy supplied by H_2 to the total energy supplied by both fuels. This parameter is commonly referred to as the hydrogen energy share (HES), and it is calculated using Equation (1).

$$HES\ (\%) = \frac{\dot{m}_{H_2} LHV_{H_2}}{\dot{m}_{H_2}\ LHV_{H_2} + \dot{m}_{diesel\ fuel}\ LHV_{diesel\ fuel}} \cdot 100, \quad (1)$$

where $\dot{m}_{H_2}$ and $\dot{m}_{\text{diesel fuel}}$ represent the mass flow rates of H_2 and diesel fuel, in kg/h, respectively. LHV_{H_2} and $LHV_{\text{diesel fuel}}$ are the lower heating values of H_2 and diesel fuel, in J/kg. However, the utilization of H_2 encounters two challenges requiring attention: knocking and backfiring. H_2 influences the combustion process, as explained subsequently. On occasion, the combustion can arise prematurely, igniting before the piston reaches the top dead center (TDC) and causing sudden vibrations. This occurrence, known as knocking, can be detected through engine vibration and the audible pinging sound caused by combustion [34,35]. It presents a significant obstacle to determining the maximum HES, as higher H_2 levels increase the likelihood of knocking. For example, Castro et al. [36] detected knocking in a marine four-cylinder diesel engine at 80% HES under all load conditions. For other operating modes, there was no evidence of knocking. Bakar et al. [37] conducted tests on a single-cylinder diesel engine using H_2 flow rates up to 49.6 L/min

and engine loads ranging from 5 to 25 Nm. In general, the higher the load, the lower the maximum amount of H_2 that can be supplemented.

Backfiring is the combustion of fresh air and H_2 during the intake process in the intake manifold or combustion chamber. When the fresh mixture enters the combustion chamber, the remaining hot residual gas can generate an ignition. This ignition is similar to pre-ignition, with the difference that pre-ignition occurs during the compression stroke, with the intake valves closed. Backfiring is an undesirable situation that occurs when the intake valves are open, and it can seriously damage the intake manifold [19]. This issue can be resolved by correctly injecting H_2 into the engine. Therefore, it is essential to select the most suitable method for combining H_2 with air.

The approach to injecting H_2 into the engine significantly impacts engine performance [38]. One main advantage of H_2 use is the ability to employ the same fuel injection methods utilized for compressed natural gas (CNG) and liquified natural gas (LNG), which include (i) carburation, (ii) inlet manifold injection, (iii) inlet port injection, and (iv) direct injection. Figure 2 provides a schematic representation of these techniques.

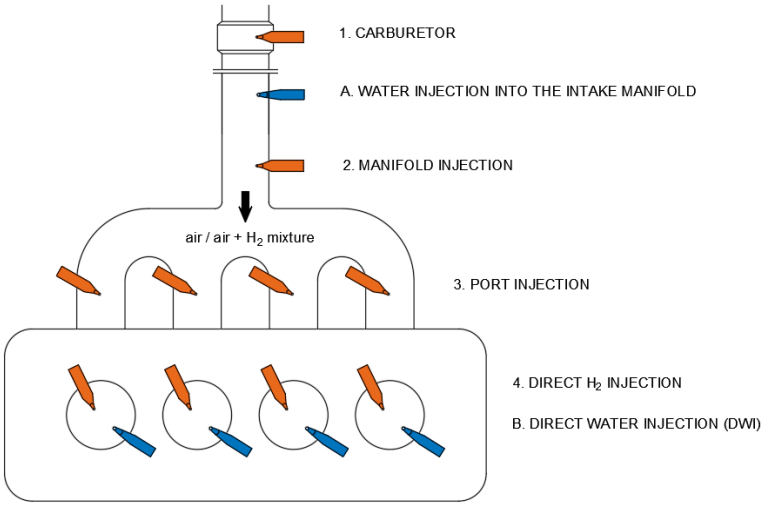

Figure 2. Schematic drawing of the different H_2 (orange) and water (blue) injection techniques.

Carburation is the earliest and most straightforward technique employed in spark ignition engines (SIEs), wherein the fuel is mixed with the air via a carburetor before it enters the intake manifold. This approach has an advantage over the methods below, as high fuel supply pressure is not required [32,39,40]. However, carburation use implies the presence of an air–H_2 mixture in the intake manifold. This remnant can pose a significant risk in CIEs if the intake valve closes and sudden ignition occurs with a premix. If the intake valve opens, the flame can spread through the intake manifold, resulting in a backfire and severely compromising the engine [32,38,40].

Injection allows for timed and precise control of H_2 input into the engine, unlike carburation, which is dependent on throttle position. At the start of the intake phase, injectors deliver H_2 into the intake manifold, leaving no remnants and decreasing the likelihood of backfire [38]. Injection can be controlled either mechanically or electronically. Electronic injectors possess a sturdy construction and offer precise control over injection timing and duration at high speeds [32,41]. Mechanical injectors are better-suited than carburation due to their sluggish response time.

As indicated earlier, three types of injections can be distinguished for hydrogen. H_2 may be injected directly into the manifold without an intermediate gas mixer. In this scenario, the fuel supply pressure will be higher compared to carburation, as there is no increase in the intake air velocity and, consequently, the air pressure is not reduced. Two methods can be identified based on the location of the H_2 injection. In port injection, the injection point is located near the intake valve, typically within a range of 10–15 mm, while

in manifold injection the distance is much higher, usually between 100 and 200 mm [41]. When dealing with a poly-cylinder engine, such as the one illustrated in Figure 2, in the case of port injection, as many injectors as cylinders must be used. Conversely, in the case of manifold injection, only one injector is required, thus simplifying the process. Port injection offers the advantage of ensuring that each cylinder contains the same amount of H_2. However, with manifold injection, this guarantee cannot be made because the size of the common rail can impact the amount delivered to each cylinder.

Saravanan and Nagarajan [35,41] conducted several studies comparing the performance and emissions of a single cylinder direct injection diesel engine with different H_2 injection techniques (carburetor, manifold, and port injection) and found that port injection provided superior performance and emissions compared to carburetor and manifold injection techniques.

Finally, in direct injection, hydrogen directly enters the combustion chamber via high-pressure direct injection (HPDI) or low-pressure direct injection (LPDI) [32]. LPDI occurs near the bottom dead center (BDC) at the end of the intake phase, while HPDI takes place after the compression phase. As the injection occurs inside the combustion chamber, the risk of backfire decreases [42]. The primary limitation of this injection technique is that the injectors are ill-equipped for the severe thermal stress it produces, particularly in high-pressure injection scenarios. As a result, this method may prove impractical, especially if significant engine modifications are unwanted [32,39,43,44]. Liu et al. [45] conducted an experiment wherein they bypassed three cylinders of a traditional four-cylinder engine and injected H_2 directly into the combustion chamber using a commercial spray-guided gasoline direct injector. Although there were no errors observed during the testing, oil needed to be added to the injector every day of testing to lubricate the injector needle.

The upcoming sections will investigate the effects of hydrogen addition on engine performance and emissions. To track trends in the analyzed parameters, a table of recent work (from 2016 onwards) will be assembled for each parameter. The studies will be categorized by engine type, starting with poly-cylinder engines (which relate more closely to transport) and then moving on to single-cylinder engines used in other sectors. For each study, additional information regarding test conditions (amount of supplied H_2, used technique, engine specifications, test speed, and load) will be provided. The main results will be analyzed to draw a conclusion regarding the effect of H_2 addition on the parameter being investigated. Findings may vary based on their design and execution. When conducting a test, certain variables, such as HES, $\dot{m}_{H_2}$, $\dot{m}_{\text{diesel fuel}}$, and engine load, will be either set or varied to achieve specific outcomes. To categorize the tests performed in the studies, various types of tests will be classified for a particular engine speed. Table 2 shows a schematic representation of the differences between each type of test:

- Type 1: In this scenario, the values of $\dot{m}_{H_2}$ and $\dot{m}_{\text{diesel fuel}}$ are adjusted to acquire the desired HES for a specific engine load. In case the HES is increased, $\dot{m}_{H_2}$ will be increased while $\dot{m}_{\text{diesel fuel}}$ will be decreased while keeping the engine speed and load constant, as before. Rocha et al. [23] kept the engine load at 60% and carried out experiments for various HESs (ranging from 0 to 24%). When no H_2 was injected (0% HES), the value of $\dot{m}_{\text{diesel fuel}}$ was recorded as 1.1072 kg/h. When the HES increased to 5%, the diesel fuel mass flow rate decreased to 1.0394 kg/h, while the hydrogen mass flow rate increased by 0.0194 kg/h. At 24% HES, the diesel fuel mass flow rate decreased to 0.9318 kg/h, while the hydrogen mass flow rate increased to 0.1021 kg/h, with no change to the initial 60% engine load.
- Type 2: When intending to maintain a constant engine load for an established $\dot{m}_{H_2}$, it is necessary to decrease $\dot{m}_{\text{diesel fuel}}$ relative to the scenario without H_2, causing a higher HES. Subsequently, with higher $\dot{m}_{\text{diesel fuel}}$ in a subsequent test, $\dot{m}_{\text{diesel fuel}}$ will be further reduced, thereby increasing the HES and keeping the previously established engine load. Yilmaz et al. [46] conducted tests at three engine loads (50, 75, and 100 Nm) and two hydrogen volumetric flow rates (20 and 40 L/min). At 75 Nm, no

H_2 injection resulted in a 0% HES, increasing up to 8.93% and 17.35%, with 20 and 40 L/min, respectively, while keeping constant the initial engine load.

- Type 3: In this case, the test is conducted at a specified speed without any hydrogen injection. The diesel fuel mass flow rate measured at this test point is kept for the remaining points, where a specified hydrogen mass flow rate is assigned, resulting in a higher fuel quantity. To maintain a constant speed, the engine load must be increased. In this sense, the authors conducted a study where the diesel fuel mass flow rate remained constant at 1500 rpm. An increase in the hydrogen mass flow rate resulted in higher hydrogen enrichment in the fuel mixture, which in turn led to greater power output and increased engine speed. To maintain a constant speed of 1500 rpm, the brake load needed to be adjusted accordingly [47].

Table 2. Summary of the types of tests.

	Engine Load	HES	$\dot{m}_{H_2}$	$\dot{m}_{\text{diesel fuel}}$
Type 1	Set out in the study	Set out in the study	Varies when modifying the HES	Varies when modifying the HES
Type 2	Set out in the study	Varies when modifying $\dot{m}_{H_2}$	Set out in the study	Varies when modifying $\dot{m}_{H_2}$
Type 3	Varies when modifying $\dot{m}_{H_2}$	Varies when modifying $\dot{m}_{H_2}$	Set out in the study	Set out in the study

HES: Hydrogen energy share.

2.1. Effect of Hydrogen as a Dual Fuel on Combustion Performance Characteristics

In this review, the main performance parameters analyzed are the brake thermal efficiency (BTE), volumetric efficiency (VE), ignition delay (ID), combustion duration (CD), and maximum in-cylinder pressure.

2.1.1. Brake Thermal Efficiency

BTE is a critical performance parameter in engine testing. Efficient use of fuel is essential for optimal engine performance. It measures the engine's ability to convert the fuel energy into power, and it is expressed as the ratio of power output to fuel energy input. For the calculation of the BTE for a dual-fuel engine, Equation (2) is used [48].

$$BTE = \frac{2\,\pi\,n\,T}{\left(\dot{m}_{H_2}\,\mathrm{LHV}_{H_2}\right) + \left(\dot{m}_{H_2}\,LHV_{diesel\ fuel}\right)}\,100, \quad (2)$$

where T represents the engine torque, in Nm; n is the engine speed, in rpm; and $\dot{m}_{H_2}$ and $\dot{m}_{\text{diesel fuel}}$ represent the mass flow rates of H_2 and diesel fuel, in kg/h, respectively. LHV_{H_2} and $\mathrm{LHV}_{\text{diesel fuel}}$ are the lower heating values of H_2 and diesel fuel, in J/kg. Table 3 highlights recent and relevant studies exploring BTE with H_2 additions.

Table 3. Results of brake thermal efficiency (BTE) with the addition of H_2.

Ref.	H_2 Enrichment and Mixing Process Type of Test	Engine Specifications	Key Findings (BTE=) Data Directly Reflected in the Document (BTE≈) Approximately Measured Data in the Document's Figures
[49]	0–25% HES Manifold inj. Type 1	Four cylinders Max. power: 103 kW at 4000 rpm Max. torque: 320 Nm at 1750–2500 rpm Turbocharged	(2000 rpm, 15% load, no H_2) BTE = 27.96% (2000 rpm, 15% load, 25% HES) BTE = 28.94% (2000 rpm, 30% load, no H_2) BTE = 35.95% (2000 rpm, 30% load, 25% HES) BTE = 34.12% (2000 rpm, 45% load, no H_2) BTE = 37.43% (2000 rpm, 45% load, 25% HES) BTE = 36.44%
[50]	25 L/min Carburetor Type 2	Four cylinders Max. power: 60 kW at 2200 rpm Max. torque: 290 Nm at 1400 rpm Naturally aspirated MEP = 0.689 MPa	(2200 rpm, 25% load, no H_2) BTE ≈ 12% (2200 rpm, 25% load, 25 L/min) BTE ≈ 13% (2200 rpm, 50% load, no H_2) BTE ≈ 16% (2200 rpm, 50% load, 25 L/min) BTE ≈ 18% (2200 rpm, 100% load, no H_2) BTE = 21.85% (2200 rpm, 100% load, 25 L/min) BTE = 23.5%

Table 3. *Cont.*

Ref.	H_2 Enrichment and Mixing Process Type of Test	Engine Specifications	Key Findings (BTE=) Data Directly Reflected in the Document (BTE≈) Approximately Measured Data in the Document's Figures
[51]	0–40 L/min Carburetor Type 2	Four cylinders Max. power: 48 kW at 4000 rpm Max. torque: 160 Nm at 1750 rpm Turbocharged	(1750 rpm, 50 Nm, no H_2) BTE = 32% (1750 rpm, 50 Nm, 20 L/min) BTE = 32% (1750 rpm, 50 Nm, 40 L/min) BTE = 32% (1750 rpm, 75 Nm, no H_2) BTE = 35% (1750 rpm, 75 Nm, 20 L/min) BTE = 35% (1750 rpm, 75 Nm, 40 L/min) BTE = 36% (1750 rpm, 100 Nm, no H_2) BTE = 38% (1750 rpm, 100 Nm, 20 L/min) BTE = 39% (1750 rpm, 100 Nm, 40 L/min) BTE = 37%
[52]	0–30% HES Direct inj. Type 1	Two cylinders Max. power: 21 kW at 2200 rpm Max. torque: No data Naturally aspirated	(1800 rpm, no H_2) BTE = 29.5% (1800 rpm, 10% HES) BTE = 30% (1800 rpm, 20% HES) BTE = 32.2% (1800 rpm, 30% HES) BTE = 35%
[21]	7 L/min Manifold inj. Type 2	Single cylinder Max. power: 5.2 kW at 1500 rpm Max. torque: No data Naturally aspirated	(1500 rpm, 30% load, no H_2) BTE ≈ 14.5% (1500 rpm, 30% load, 7 L/min) BTE ≈ 15% (1500 rpm, 50% load, no H_2) BTE ≈ 21% (1500 rpm, 50% load, 7 L/min) BTE ≈ 22% (1500 rpm, 100% load, no H_2) BTE ≈ 26% (1500 rpm, 100% load, 7 L/min) BTE ≈ 26.5%
[53]	0–10 L/min (0–28% HES) Manifold inj. Type 2	Single cylinder Max. power: 5.2 kW at 1500 rpm Max. torque: No data Naturally aspirated	(1500 rpm, 30% load, no H_2) BTE ≈ 13% (1500 rpm, 30% load, 7 L/min) BTE ≈ 18% (1500 rpm, 30% load, 10 L/min) BTE ≈ 17% (1500 rpm, 90% load, no H_2) BTE ≈ 26% (1500 rpm, 90% load, 7 L/min) BTE ≈ 32% (1500 rpm, 90% load, 10 L/min) BTE ≈ 30% (1500 rpm, 100% load, no H_2) BTE ≈ 25% (1500 rpm, 100% load, 7 L/min) BTE ≈ 30% (1500 rpm, 100% load, 10 L/min) BTE ≈ 27.5%
[54]	0–30% HES Manifold inj. Type 1	Single cylinder Max. power: 5.2 kW at 1500 rpm Max. torque: No data Naturally aspirated	(1500 rpm, 25% load, no H_2) BTE ≈ 15% (1500 rpm, 25% load, 30% HES) BTE ≈ 14% (1500 rpm, 50% load, no H_2) BTE ≈ 20.5% (1500 rpm, 50% load, 30% HES) BTE ≈ 20.5% (1500 rpm, 100% load, no H_2) BTE ≈ 29% (1500 rpm, 100% load, 30% HES) BTE ≈ 31%
[22]	0–0.08 kg/h (0–28% HES) Port inj. Type 2	Single cylinder Max. power: 7.4 kW at 3600 rpm Max. torque: 28 Nm at 2000 rpm Naturally aspirated	(1800 rpm, 10 Nm, no H_2) BTE = 20.78% (1800 rpm, 10 Nm, 7.5% HES) BTE ≈ 20.4% (1800 rpm, 10 Nm, 17.5% HES) BTE ≈ 19.5% (1800 rpm, 10 Nm, 28% HES) BTE = 19.59%
[55]	0–20% HES Manifold inj. Type 1	Single cylinder Max. power: 5.2 kW at 1500 rpm Max. torque: No data Naturally aspirated	(1500 rpm, 25% load, no H_2) BTE ≈ 16% (1500 rpm, 25% load, 10% HES) BTE ≈ 16% (1500 rpm, 25% load, 20% HES) BTE ≈ 15.5% (1500 rpm, 50% load, no H_2) BTE ≈ 24.5% (1500 rpm, 50% load, 10% HES) BTE ≈ 23.7% (1500 rpm, 50% load, 20% HES) BTE ≈ 23.5% (1500 rpm, 75% load, no H_2) BTE ≈ 28.2% (1500 rpm, 75% load, 10% HES) BTE ≈ 28% (1500 rpm, 75% load, 20% HES) BTE ≈ 27.5%
[56]	0–36 L/min (0–86% HES) Manifold inj. Type 2	Single cylinder Max. power: 5.97 kW at 2200 rpm Max. torque: No data Naturally Aspirated	(1850 rpm, 4 Nm load, no H_2) BTE ≈ 13% (1850 rpm, 4 Nm load, 6 L/min) BTE ≈ 13% (1850 rpm, 4 Nm load, 18 L/min) BTE ≈ 10% (1850 rpm, 4 Nm load, 36 L/min) BTE ≈ 10% (1850 rpm, 20 Nm load, no H_2) BTE ≈ 31% (1850 rpm, 20 Nm load, 6 L/min) BTE ≈ 29.5% (1850 rpm, 20 Nm load, 18 L/min) BTE ≈ 29% (1850 rpm, 20 Nm load, 36 L/min) BTE ≈ 29%

HES: Hydrogen energy share.

For conventional vehicle engines used in commercial applications, numerous studies have demonstrated that the incorporation of H_2 enables a positive impact on the BTE across all load ranges. Hoang and Pham [50], Yilmaz and Gumus [51], and Wu et al. [52] reported

an improvement in the combustion process, which increased the BTE, due to H_2's high diffusivity and flame propagation. Barrios et al. [49], however, did not find a clear trend, arguing that the lack of EGR control would influence the combustion process.

There appears to be a disparity in results concerning lower-powered engines. Das et al. [53] and Kanth and Debbarma [21] found similar tendencies to those described above for more powerful engines based on the same facts. However, Nag et al. [54] concluded that the use of H_2 has a positive effect on BTE, except for low loads, as the lower combustion efficiency of H_2 causes a drop. Studies conducted by Sharma and Dhar [55] and Subramanian and Thangavel [56] suggested that at medium and high loads, the BTE also decreased. The reason for this is that the wall heat flux of the H_2 flame was found to be higher than that of diesel fuel, which results in higher thermal losses and, consequently, lower BTE [57]. Furthermore, Pinto et al. [22] reported that during a medium load, the reduction in BTE occurs because the prolonged ignition delay causes a significant portion of the fuel to burn during the expansion stroke. They concluded that modifying the pilot fuel injection is necessary to reduce this inefficient behavior.

Several studies, including those by Yilmaz and Gumus [51] and Das et al. [53], have suggested that the higher the HES, the lower the BTE. This could be due to the displacement of O_2 by H_2 in the intake manifold. These findings have been observed in both large and small engines, although other research indicates the opposite trend, stating that the higher the HES levels, the higher the BTE [21,53]. The displacement may also be impacted in naturally aspirated engines. Most of the engines for commercial use are turbocharged, whereby the air enters at a higher pressure and reduces the displacement.

2.1.2. Volumetric Efficiency

VE is a metric that gauges the breathing efficiency of an engine. It gives the proportion of the volume of fresh air taken into the engine cylinder prior to the intake valves, with shutting relative to the cylinder-swept volume at atmospheric conditions (1 atm and 298 K) [58]. VE can be calculated using Equation (3) [23].

$$\eta_v = \frac{2\dot{m}_{air}}{\rho_{air}\, V_d}, \tag{3}$$

where the mass flow of air is represented by $\dot{m}_{air}$ and ρ_{air} is the density of air calculated using the temperature and the pressure of the air within the intake manifold, in kg/h and kg/m^3, respectively. V_d represents the displaced volume in m^3. Table 4 presents recent relevant studies analyzing VE with the addition of H_2.

Table 4. Results of volumetric efficiency (VE) with the addition of H_2.

Ref.	H_2 Enrichment and Mixing Process Type of Test	Engine Specifications	Key Findings (VE=) Data Directly Reflected in the Document (VE≈) Approximately Measured Data in the Document's Figures
[23]	0–10% mass fraction (0–24% HES) Manifold inj. Type 2	Single cylinder Max. power: 7.35 kW at 3600 rpm Max. torque: No data Naturally aspirated	(3600 rpm, 60% load, no H_2) VE = 79.9% (3600 rpm, 60% load, 2% mass) VE = 79.5% (3600 rpm, 60% load, 6% mass) VE = 78.7% (3600 rpm, 60% load, 8% mass) VE = 77% (3600 rpm, 60% load, 10% mass) VE = 75.4%
[54]	0–30% HES Manifold inj. Type 1	Single cylinder Max. power: 5.2 kW at 1500 rpm Max. torque: No data Naturally aspirated	(1500 rpm, 25% load, no H_2) VE ≈ 68.5% (1500 rpm, 25% load, 10% HES) VE ≈ 67.5% (1500 rpm, 25% load, 30% HES) VE ≈ 67% (1500 rpm, 50% load, no H_2) VE ≈ 67% (1500 rpm, 50% load, 10% HES) VE ≈ 66.5% (1500 rpm, 50% load, 30% HES) VE ≈ 65.5% (1500 rpm, 100% load, no H_2) VE ≈ 65.5% (1500 rpm, 100% load, 10% HES) VE ≈ 64% (1500 rpm, 100% load, 30% HES) VE ≈ 62%

Table 4. *Cont.*

Ref.	H_2 Enrichment and Mixing Process Type of Test	Engine Specifications	Key Findings (VE=) Data Directly Reflected in the Document (VE≈) Approximately Measured Data in the Document's Figures
[55]	0–20% HES Manifold inj. Type 1	Single cylinder Max. power: 5.2 kW at 1500 rpm Max. torque: No data Naturally aspirated	(1500 rpm, 50% load, no H_2) VE = 75.8% (1500 rpm, 50% load, 10% HES) VE = 74.8% (1500 rpm, 50% load, 20% HES) VE = 73.9% (1500 rpm, 75% load, no H_2) VE = 75.6% (1500 rpm, 75% load, 10% HES) VE = 73.7% (1500 rpm, 75% load, 20% HES) VE = 72.2%
[56]	0–36 L/min (0–86% HES) Manifold inj. Type 2	Single cylinder Max. power: 5.97 kW at 2200 rpm Max. torque: No data	(1850 rpm, 20 Nm, 6 L/min) BTE = 8.8% higher than 36 lpm

HES: Hydrogen energy share.

Only single-cylinder-engine studies have been found for VE calculation. In all cases, the use of hydrogen led to a reduction in VE at all load rates due to hydrogen's lower density than air. This resulted in a significant displacement of air when introducing it into the combustion chamber. Nag et al. [54], Rocha et al. [23], Sharma et al. [55], and Subramanian et al. [56] noted that the higher the HES, the lower the VE. This reduction arises from a greater amount of air being replaced by H_2 in the combustion chamber.

2.1.3. Ignition Delay

ID is defined as the time between the start of fuel injection into the cylinder (SOI) and the start of combustion (SOC) [59]. This time can be measured as the difference between the crank angle where 0% and 10% of heat are released. The delay period consists of a physical and a chemical delay that occur simultaneously [59]. Fuel properties and composition are responsible for the physical delay [60], while the chemical delay is dependent on the cylinder temperature, cylinder pressure, and fuel properties [61]. Table 5 shows some of the most relevant recent studies in which ID is studied with the addition of H_2.

Table 5. Results of ignition delay (ID) with the addition of H_2.

Ref.	H_2 Enrichment and Mixing Process Type of Test	Engine Specifications	Key Findings (ID=) Data Directly Reflected in the Document (ID≈) Approximately Measured Data in the Document's Figures
[46]	0–40 L/min (0–24% HES) Carburetor Type 2	Four cylinders Max. power: 48 kW at 4000 rpm Max. torque: 160 Nm at 1750 rpm Turbocharged	(1750 rpm, 50 Nm, no H_2) ID = 17° CA (1750 rpm, 50 Nm, 20 L/min) ID = 26° CA (1750 rpm, 50 Nm, 40 L/min) ID = 25° CA (1750 rpm, 75 Nm, no H_2) ID = 26° CA (1750 rpm, 75 Nm, 20 L/min) ID = 29° CA (1750 rpm, 75 Nm, 40 L/min) ID = 28° CA (1750 rpm, 100 Nm, 0, 20, 40 L/min) ID = 27° CA
[62]	0–50% HES Carburetor Type 1	Four cylinders Max. power: 62.5 kW at 1500 rpm Max. torque: No data Turbocharged	(1500 rpm, 13% load, no H_2) ID = 11° CA (1500 rpm, 13% load, 30% HES) ID = 13° CA (1500 rpm, 13% load, 50% HES) ID = 11° CA (1500 rpm, 40% load, no H_2) ID = 9° CA (1500 rpm, 40% load, 30% HES) ID = 10.5° CA (1500 rpm, 40% load, 50% HES) ID = 9.5° CA (1500 rpm, 80% load, no H_2) ID = 8° CA (1500 rpm, 80% load, 30% HES) ID = 9.5° CA (1500 rpm, 80% load, 50% HES) ID = 9° CA
[63]	0–50% HES Carburetor Type 1	Four cylinders Max. power: 62.5 kW at 1500 rpm Max. torque: No data Turbocharged	(1500 rpm, 40% load, no H_2) ID = 10° CA (1500 rpm, 40% load, 30% HES) ID = 13° CA (1500 rpm, 40% load, 50% HES) ID = 10° CA (1500 rpm, 80% load, no H_2) ID = 9° CA (1500 rpm, 80% load, 30% HES) ID = 11° CA (1500 rpm, 80% load, 50% HES) ID = 9° CA

Table 5. *Cont.*

Ref.	H_2 Enrichment and Mixing Process Type of Test	Engine Specifications	Key Findings (ID=) Data Directly Reflected in the Document (ID≈) Approximately Measured Data in the Document's Figures
[23]	0–10% mass fraction (0–24% HES) Manifold inj. Type 2	Single cylinder Max. power: 7.35 kW at 3600 rpm Max. torque: No data Naturally aspirated	(3600 rpm, 60% load, no H_2) ID = 15.68° CA (3600 rpm, 60% load, 2% mass) ID = 15.34° CA (3600 rpm, 60% load, 6% mass) ID = 15.24° CA (3600 rpm, 60% load, 8% mass) ID = 15.15° CA (3600 rpm, 60% load, 10% mass) ID = 15.03° CA
[24]	0–34% HES Manifold inj. Type 1	Single cylinder Max. power: 7 kW at 1500 rpm Max. torque: No data Naturally aspirated	(1500 rpm, 100% load, no H_2) ID = 18° CA (1500 rpm, 100% load, 4% HES) ID = 18° CA (1500 rpm, 100% load, 7% HES) ID = 18° CA (1500 rpm, 100% load, 12% HES) ID = 18° CA (1500 rpm, 100% load, 23% HES) ID = 19° CA (1500 rpm, 100% load, 34% HES) ID = 18° CA
[53]	0–10 L/min (0–28% HES) Manifold inj. Type 2	Single cylinder Max. power: 5.2 kW at 1500 rpm Max. torque: 84.4 Nm at 1200 rpm Naturally aspirated	(1500 rpm, 30% load, no H_2) ID = 7° CA (1500 rpm, 30% load, 10 L/min) ID = 8° CA (1500 rpm, 60% load, no H_2) ID = 6° CA (1500 rpm, 60% load, 10 L/min) ID = 7° CA (1500 rpm, 90% load, no H_2) ID = 5° CA (1500 rpm, 90% load, 10 L/min) ID = 7° CA
[22]	0–0.08 kg/h (0–28% HES) Port inj. Type 2	Single cylinder Max. power: 7.4 kW at 3600 rpm Max. torque: 28 Nm at 2000 rpm Naturally aspirated	(1800 rpm, 10 Nm, no H_2) ID ≈ 12.5° CA (1800 rpm, 10 Nm, 7.37% HES) ID ≈ 12.8° CA (1800 rpm, 10 Nm, 17.52% HES) ID ≈ 12.9° CA (1800 rpm, 10 Nm, 28.60% HES) ID =13.03° CA
[64]	0–50% HES Manifold inj. Type 2	Single cylinder Max. power: 13.2 kW at 1500 rpm Max. torque: No data Naturally aspirated	(965 rpm, ML, no H_2) ID = 22° CA (965 rpm, ML, 15% HES) ID = 21° CA (965 rpm, ML, 41% HES) ID = 17° oCA (965 rpm, NL, no H_2) ID = 20° CA (965 rpm, NL, 14% HES) ID = 21° CA (965 rpm, NL, 33% HES) ID = 15° CA

HES: hydrogen energy share, ML: medium load, NL: nominal load.

For commercial engines that can be used in conventional vehicles, research has shown that using H_2 can cause ID. Dhole et al. [62] revealed that higher mixture-specific heat (C_p) and fewer ignition sources are responsible for reducing the temperature of the gaseous fuel–air mixture at low and medium loads (13% and 40%). This results in an increased ID compared to the diesel mode (2° CA). At 80% load, they observed that higher temperatures promote increased heat transfer to diesel fuel droplets. This resulted in faster evaporation and a smaller ID compared to low and medium load cases, but they were still higher than the diesel fuel mode (1.5° CA). Similar results were obtained by Lata et al. [63] at 10%, 40%, and 80% loads with IDs of 4, 3, and 2° CA, respectively. Yilmaz et al. [46] reported a significant ID when introducing H_2 at 50 Nm (9° CA with respect to the diesel fuel case). However, this delay was reduced as the engine load increased (by 3° CA at 75 Nm and by a non-negligible amount at 100 Nm). The authors argued that ignition of the pilot fuel may be affected by the reaction with the air–H_2 mixture. However, all studies have shown a consistent trend in the impact of HES on ID. At higher HES levels, the delay is reduced until values are equal to those of the diesel fuel case. Dhole et al. [62] noted that with a higher HES at a high load, flame propagation from multiple ignition centers of the pilot fuel was rapid and consumed the majority of the air–H_2 mixture, leading to higher residual gas temperature and consequently reducing ID.

There seems to be a discrepancy in results for lower-powered engines. Das et al. [53] and Pinto et al. [22] reported a similar trend as above for more powerful engines, but with different explanations. Das et al. [53] stated that the increase in delay (1–2° CA) is due to H_2's high auto-ignition temperature, which causes the air–H_2 mixture to ignite more slowly. Pinto et al. [22] argued that there was a delay of 0.5° CA. This resulted from the lesser quantity of pilot fuel injected under the dual-fuel mode, which was replaced by H_2. Nevertheless, contrasting with this claim are the findings of Juknelevicius et al. [64]

and Rocha et al. [23], who reported that H_2 speeds up the combustion of the blended fuel, thereby advancing the combustion initiation by 5° CA and 0.5° CA, which is the opposite of the findings mentioned above. Finally, Tutak et al. [24] found no significant differences between net diesel fuel operation mode and dual-fuel operation mode.

2.1.4. Combustion Duration

CD is the time span between the start and end of combustion in relation to the crank angle. It is measured by calculating the difference between the crank angle at which 10% and 90% of the heat are released [53]. Decreasing CD has a positive impact on engine operations, as it restricts the amount of heat released to the cylinder and combustion chamber walls, thus boosting efficiency. In addition, it promotes reduced knocking and improved combustion, leading to lower HC emissions. In addition to the mentioned benefits, faster fuel burn also results in rough engine operation (higher pressure rise rate for one degree of rotation of the crankshaft). Table 6 illustrates recent studies exploring CD with the addition of H_2.

Table 6. Results of combustion duration (CD) with the addition of H_2.

Ref.	H_2 Enrichment and Mixing Process Type of Test	Engine Specifications	Key Findings (CD=) Data Directly Reflected in the Document (CD≈) Approximately Measured Data in the Document's Figures
[46]	0–40 L/min Carburetor Type 2	Four cylinders Max. power: 48 kW at 4000 rpm Max. torque: 160 Nm at 1750 rpm Turbocharged	(1750 rpm, 50 Nm, no H_2) CD = 66° CA (1750 rpm, 50 Nm, 20 L/min) CD = 90° CA (1750 rpm, 50 Nm, 40 L/min) CD = 95° CA (1750 rpm, 75 Nm, no H_2) CD = 87° CA (1750 rpm, 75 Nm, 20 L/min) CD = 88° CA (1750 rpm, 75 Nm, 40 L/min) CD = 91° CA (1750 rpm, 100 Nm, no H_2) CD = 92° CA (1750 rpm, 100 Nm, 20 L/min) CD = 89° CA (1750 rpm, 100 Nm, 40 L/min) CD = 89° CA
[62]	0–50% HES Carburetor Type 1	Four cylinders Max. power: 62.5 kW at 1500 rpm Max. torque: No data Turbocharged	(1500 rpm, 13% load, no H_2) CD = 23° CA (1500 rpm, 13% load, 30% HES) CD = 25.5° CA (1500 rpm, 13% load, 50% HES) CD = 24° CA (1500 rpm, 40% load, no H_2) CD = 25° CA (1500 rpm, 40% load, 30% HES) CD = 24° CA (1500 rpm, 40% load, 50% HES) CD = 23° CA (1500 rpm, 80% load, no H_2) CD = 30° CA (1500 rpm, 80% load, 30% HES) CD = 27.5° CA (1500 rpm, 80% load, 50% HES) CD = 26° CA
[24]	0–34% HES Manifold inj. Type 1	Single cylinder Max. power: 7 kW at 1500 rpm Max. torque: No data Naturally aspirated	(1500 rpm, 100% load, no H_2) CD = 53° CA (1500 rpm, 100% load, 4% HES) CD = 52° CA (1500 rpm, 100% load, 7% HES) CD = 49° CA (1500 rpm, 100% load, 12% HES) CD = 47° CA (1500 rpm, 100% load, 23% HES) CD = 43° CA (1500 rpm, 100% load, 34% HES) CD = 52° CA
[53]	0–10 L/min (0–28% HES) Manifold inj. Type 2	Single cylinder Max. power: 5.2 kW at 1500 rpm Max. torque: 84.4 Nm at 1200 rpm Naturally aspirated	(1500 rpm, 30% load, no H_2) CD ≈ 26° CA (1500 rpm, 30% load, 10 L/min) CD ≈ 27° CA (1500 rpm, 90% load, no H_2) CD ≈ 30° CA (1500 rpm, 90% load, 10 L/min) CD ≈ 28° CA (1500 rpm, 100% load, no H_2) CD ≈ 32° CA (1500 rpm, 100% load, 10 L/min) CD ≈ 28° CA
[22]	0–0.08 kg/h (0–28% HES) Port inj. Type 2	Single cylinder Max. power: 7.4 kW at 3600 rpm Max. torque: 28 Nm at 2000 rpm Naturally aspirated	(1800 rpm, 10 Nm, no H_2) CD = 26.66° CA (1800 rpm, 10 Nm, 7.5% HES) CD ≈ 25.5° CA (1800 rpm, 10 Nm, 17.5% HES) CD ≈ 22.2° CA (1800 rpm, 10 Nm, 28% HES) CD = 22.66° CA

Table 6. *Cont.*

Ref.	H_2 Enrichment and Mixing Process Type of Test	Engine Specifications	Key Findings (CD=) Data Directly Reflected in the Document (CD≈) Approximately Measured Data in the Document's Figures
[56]	0–36 L/min (0–86% HES) Manifold inj. Type 2	Single cylinder Max. power: 5.97 kW at 2200 rpm Max. torque: No data	(1850 rpm, 4 Nm load, no H_2) CD ≈ 30° CA (1850 rpm, 4 Nm load, 6 L/min) CD ≈ 33° CA (1850 rpm, 4 Nm load, 18 L/min) CD ≈ 32° CA (1850 rpm, 4 Nm load, 36 L/min) CD ≈ 33° CA (1850 rpm, 20 Nm load, no H_2) CD ≈ 38° CA (1850 rpm, 20 Nm load, 6 L/min) CD ≈ 45 ° CA (1850 rpm, 20 Nm load, 18 L/min) CD ≈ 58° CA (1850 rpm, 20 Nm load, 36 L/min) CD ≈ 61° CA
[64]	0–50% HES Manifold inj. Type 2	Single cylinder Max. power: 13.2 kW at 1500 rpm Max. torque: No data Naturally aspirated	(965 rpm, ML, no H_2) CD ≈ 65° CA (965 rpm, ML, 15% HES) CD ≈ 58° CA (965 rpm, ML, 41% HES) CD ≈ 56° CA (965 rpm, NL, no H_2) CD ≈ 70° CA (965 rpm, NL, 14% HES) CD ≈ 66° CA (965 rpm, NL, 33% HES) CD ≈ 56° CA

HES: hydrogen energy share, ML: medium load, NL: nominal load.

Studies have shown that for commercial engines used in conventional vehicles, hydrogen can have both positive and negative effects on CD, depending on the engine load. According to Dhole et al. [62], at a low load (13%), lean mixtures lead to fewer ignition centers being formed. However, the addition of H_2 reduces diesel fuel and increases CD (by 2.5° CA). At higher levels of HES, CD decreases by 1.5° CA when transitioning from 30% to 50% HES. It is suggested that this decrease could be attributed to the higher flame velocity of H_2. At higher loads, increased fuel quantity for the pilot enhances the ignition of H_2, which has a higher laminar velocity and results in decreased CD (up to 4° CA). Yilmaz et al. [46] obtained similar results with a 29° CA increase in CD compared to diesel-fuel-only mode at a 50 Nm load. It should be noted that there is a discrepancy in how the SOC is interpreted by these authors. Dhole et al. [62] define the SOC as the minimum point in cumulative heat release, whereas Yilmaz et al. [46] define it as the point where the maximum rate of pressure rise occurs.

Results differ between low- and high-powered engines, as the majority of the consulted studies indicate that CD decreases at all load rates with low-powered engines. Das et al. [53] and Juknelevicius et al. [64], over a range of loads, as well as Pinto et al. [22] at medium load and Tutak et al. [24] at full load, reported that hydrogen leads to a lower CD. Das et al. [53] reported that hydrogen forms a homogeneous mixture with air, leading to an increased combustion rate and greater fuel burned in the premixed phase. Furthermore, Pinto et al. [22] analyzed the CA in both premixed and diffusive phases and found that the addition of hydrogen resulted in shorter CA values (5.77° and 16.87° CA with hydrogen compared to 6.29° and 20.37° CA without hydrogen in the premixed and diffusive phases, respectively). They argue that hydrogen leads to higher combustion rates due to the greater flame velocity, resulting in quicker and more efficient mixing of fuels. In contrast, the study conducted by Subramanian and Thangavel [56] found that the addition of hydrogen led to a higher CD. The authors suggested that introducing hydrogen reduces the concentration of air available for combustion, thus slowing down the diffusion combustion process. This stands in stark contrast to the reasoning provided by other authors.

2.1.5. Maximum In-Cylinder Pressure

The quantity of fuel burned during premixed combustion determines the maximum in-cylinder pressure in CI engines. A richer fuel–air mixture results in a higher maximum pressure. Research on CI engine performance relies on pressure variations in the operating cycle. The maximum in-cylinder pressure increases with the engine load due to higher temperatures at higher engine loads [60]. Table 7 displays significant recent studies investigating maximum in-cylinder performance with the application of H_2.

Table 7. Results of in-cylinder pressure with the addition of H_2.

Ref.	H_2 Enrichment and Mixing Process Type of Test	Engine Specifications	Key Findings (P_{max}=) Data Directly Reflected in the Document ($P_{max}\approx$) Approximately Measured Data in the Document's Figures
[49]	0–25% HES Manifold inj. Type 1	Four cylinders Max. power: 103 kW at 4000 rpm Max. torque: 320 Nm at 1750–2500 rpm Turbocharged	(2000 rpm, 15% load, no H_2) P_{max} = 50.74 bar (2000 rpm, 15% load, 25% HES) P_{max} = 52.25 bar (2000 rpm, 45% load, no H_2) P_{max} = 71.93 bar (2000 rpm, 45% load, 25% HES) P_{max} = 69.97 bar
[51]	0–40 L/min Carburetor Type 2	Four cylinders Max. power: 48 kW at 4000 rpm Max. torque: 160 Nm at 1750 rpm Turbocharged	(1750 rpm, 50 Nm, no H_2) P_{max} = 65.7 bar (1750 rpm, 50 Nm, 20 L/min) P_{max} = 66.7 bar (1750 rpm, 50 Nm, 40 L/min) P_{max} = 73 bar (1750 rpm, 100 Nm, no H_2) P_{max} = 93 bar (1750 rpm, 100 Nm, 20 L/min) P_{max} = 94 bar (1750 rpm, 100 Nm, 40 L/min) P_{max} = 94 bar
[65]	0–21% HES Manifold inj. Type 1	Four cylinders Max. power: 55 kW at 3900 rpm Max. torque: 156 Nm at 2000 rpm Turbocharged	(2000 rpm, 55% load, no H_2) $P_{max} \approx$ 82 bar (2000 rpm, 55% load, 7% HES) $P_{max} \approx$ 90 bar (2000 rpm, 55% load, 13% HES) $P_{max} \approx$ 92 bar (2000 rpm, 55% load, 21% HES) $P_{max} \approx$ 98 bar
[21]	7 L/min Manifold inj. Type 1	Single cylinder Max. power: 5.2 kW at 1500 rpm Max. torque: No data Naturally aspirated	(1500 rpm, 100% load, no H_2) P_{max} = 61.26 bar (1500 rpm, 100% load, 7 L/min) P_{max} = 68.72 bar
[23]	0–10% HES Manifold inj. Type 2	Single cylinder Max. power: 7.35 kW at 3600 rpm Max. torque: No data Naturally aspirated	(3600 rpm, 60% load, no H_2) P_{max} = 56.1 bar (3600 rpm, 60% load, 2% HES) P_{max} = 57.4 bar (3600 rpm, 60% load, 8% HES) P_{max} = 59.1 bar (3600 rpm, 60% load, 10% HES) P_{max} = 61.2 bar
[24]	0–34% HES Manifold inj. Type 1	Single cylinder Max. power: 7 kW at 4200 rpm Max. torque: No data Naturally aspirated	(1500 rpm, 100% load, no H_2) $P_{max} \approx$ 60 bar (1500 rpm, 100% load, 34% HES) P_{max} = 71 bar
[53]	0–10 L/min (0–28% HES) Manifold inj. Type 2	Single cylinder Max. power: 5.2 kW at 1500 rpm Max. torque: 84.4 Nm at 1200 rpm Naturally aspirated	(1500 rpm, 100% load, no H_2) P_{max} = 69 bar (1500 rpm, 100% load, 7 L/min) P_{max} = 77.69 bar (1500 rpm, 100% load, 10 L/min) $P_{max} \approx$ 76 bar
[22]	0–0.08 kg/h (0–28% HES) Port inj. Type 2	Single cylinder Max. power: 7.4 kW at 3600 rpm Max. torque: 28 Nm at 2000 rpm Naturally aspirated	(1800 rpm, 10 Nm, no H_2) P_{max} = 70.69 bar (1800 rpm, 10 Nm, 7.5% HES) $P_{max} \approx$ 71 bar (1800 rpm, 10 Nm, 17.5% HES) $P_{max} \approx$ 72 bar (1800 rpm, 10 Nm, 28% HES) P_{max} = 79.89 bar
[56]	0–36 L/min (0–86% HES) Manifold inj. Type 2	Single cylinder Max. power: 5.97 kW at 2200 rpm Max. torque: No data	(1850 rpm, 20 Nm load, no H_2) $P_{max} \approx$ 59 bar (1850 rpm, 20 Nm load, 6 L/min) $P_{max} \approx$ 58.5 bar (1850 rpm, 20 Nm load, 18 L/min) $P_{max} \approx$ 54 bar (1850 rpm, 20 Nm load, 36 L/min) $P_{max} \approx$ 51 bar
[64]	0–50% HES Manifold inj. Type 2	Single cylinder Max. power: 13.2 kW at 1500 rpm Max. torque: No data Naturally aspirated	(965 rpm, ML, no H_2) P_{max} = 58 bar (965 rpm, ML, 15% HES) P_{max} = 56 bar (965 rpm, ML, 41% HES) P_{max} = 64 bar (965 rpm, NL, no H_2) P_{max} = 65.5 bar (965 rpm, NL, 14% HES) P_{max} = 65.5 bar (965 rpm, NL, 33% HES) P_{max} = 78 bar
[66]	0–15 L/min Manifold inj. Type 2	Single cylinder Max. power: 5.2 kW at 1500 rpm Max. torque: No data Naturally aspirated	(1500 rpm, 100% load, no H_2) P_{max} = 65.12 bar (1500 rpm, 100% load, 3 L/min) P_{max} = 65.77 bar (1500 rpm, 100% load, 9 L/min) P_{max} = 67.79 bar (1500 rpm, 100% load, 15 L/min) P_{max} = 70.98 bar

HES: hydrogen energy share, ML: medium load, NL: nominal load.

For commercial engines in conventional vehicles, studies demonstrate that introducing H_2 to the fuel's composition causes a rise in the maximum in-cylinder pressure. Cernat et al. [65] indicated that hydrogen's high burning velocity and calorific value result in increased heat generation in the initial combustion stages. It correspondingly contributes to an enhanced rate of maximum pressure in the premixing. Yilmaz and Gumus [51] reported that hydrogen combustion is practically instantaneous due to its high burning velocity and high diffusivity. It results in a more homogeneous fuel–air mixture. As a result,

the maximum in-cylinder pressure increased with the addition of hydrogen. In contrast, Barrios et al. [49] did not observe a clear trend and suggested that the uncontrolled EGR system may have had an effect on the combustion process.

For lower-powered engines, most authors observed a rise in the maximum in-cylinder pressure, which was explained similarly to studies with more powerful engines. However, Das et al. [53] brought attention to a reduction in the maximum in-cylinder pressure when hydrogen was at its maximum level of supply (10 L/min) compared to the case with a 7 L/min supply. They argued that hydrogen with a higher concentration consumes more oxygen, giving less oxygen for the complete combustion of diesel fuel. Even so, the maximum pressure in the hydrogen mode is higher than that in the diesel fuel mode. However, as reported by Subramanian and Thangavel [56], the absence of oxygen in the combustion process leads to a decrease in the maximum in-cylinder pressure. This confirms previous findings by Das et al. [53] but also applies to all levels of H_2 supplementation.

The high diffusivity of hydrogen produces a homogeneous air–hydrogen mixture. This mixture, along with hydrogen's high calorific value, lead to a higher heat release rate in the premix phase. The resulting increase leads to a higher maximum cylinder pressure, which grows with higher loads and increased hydrogen supply. An increase in load leads to a higher amount of fuel present in the chamber. As the amount of H_2 in the fuel mix is higher than that of the diesel fuel, the maximum pressure increases in parallel. This observed increase in pressure has been consistent across engines of all sizes.

2.2. Effect of Hydrogen as a Dual Fuel on Emission Characteristics

The complete combustion of a hydrocarbon and the oxygen in the air produces CO_2 and H_2O. However, in a CI engine, combustion is incomplete, resulting in the formation of additional products for various reasons [67,68].

- The chemical reactions are not able to complete at high engine speeds, leading to the generation of CO and HC.
- Elevated temperatures in the combustion chamber, under conditions of excess air, facilitate air oxidation, leading to the formation of NO_x.
- Situations with insufficient oxygen and excess fuel result in incomplete evaporation and carbonization of some fuel, causing the formation of PM.
- Fuel impurities can also produce SO_x.

In the following sections, the results of CO_2, CO, HC, soot, and NO_x are shown.

2.2.1. CO_2 Emissions

CO_2 is a colorless and odorless gas that results from the complete oxidation of carbon found in carbon-based fuels. It is crucial to control the emission of this gas, as it is a GHG contributing to climate change. The amount of CO_2 emitted, and the type of fuel used, are interrelated. Table 8 displays some of the most important recent studies that examine CO_2 emissions with the addition of H_2.

Table 8. Results of CO_2 emissions with the addition of H_2.

Ref.	H_2 Enrichment and Mixing Process Type of Test	Engine Specifications	Key Findings (CO_2=) Data Directly Reflected in the Document (CO_2≈) Approximately Measured Data in the Document's Figures
[36]	0–80% HES Manifold inj. Type 1	Four cylinders Max. power: 58 kW at 4500 rpm Max. torque: 145 Nm at 2350 rpm Turbocharged	(2400 rpm, 30% load, no H_2) $CO_2 \approx 950$ g/kWh (2400 rpm, 30% load, 30% HES) $CO_2 \approx 900$ g/kWh (2400 rpm, 30% load, 80% HES) $CO_2 \approx 500$ g/kWh (2400 rpm, 60% load, no H_2) $CO_2 \approx 700$ g/kWh (2400 rpm, 60% load, 30% HES) $CO_2 \approx 600$ g/kWh (2400 rpm, 60% load, 60% HES) $CO_2 \approx 400$ g/kWh (2400 rpm, 100% load, no H_2) $CO_2 \approx 650$ g/kWh (2400 rpm, 100% load, 30% HES) $CO_2 \approx 500$ g/kWh (2400 rpm, 100% load, 40% HES) $CO_2 \approx 450$ g/kWh

Table 8. *Cont.*

Ref.	H_2 Enrichment and Mixing Process Type of Test	Engine Specifications	Key Findings (CO_2=) Data Directly Reflected in the Document (CO_2≈) Approximately Measured Data in the Document's Figures
[49]	0–25% HES Manifold inj. Type 1	Four cylinders Max. power: 103 kW at 4000 rpm Max. torque: 320 Nm at 1750–2500 rpm Turbocharged	(2000 rpm, 15% load, no H_2) CO_2 = 6.09% vol (2000 rpm, 15% load, 25% HES) CO_2 = 5.03% vol (2000 rpm, 30% load, no H_2) CO_2 = 7.36% vol (2000 rpm, 30% load, 25% HES) CO_2 = 6.58% vol (2000 rpm, 45% load, no H_2) CO_2 = 7.92% vol (2000 rpm, 45% load, 25% HES) CO_2 = 7.15% vol
[51]	0–40 L/min Carburetor Type 2	Four cylinders Max. power: 48 kW at 4000 rpm Max. torque: 160 Nm at 1750 rpm Turbocharged	(1750 rpm, 50 Nm, no H_2) CO_2 ≈ 5.1% vol (1750 rpm, 50 Nm, 20 L/min) CO_2 ≈ 4.5% vol (1750 rpm, 50 Nm, 40 L/min) CO_2 ≈ 4.4% vol (1750 rpm, 100 Nm, no H_2) CO_2 ≈ 9.7% vol (1750 rpm, 100 Nm, 20 L/min) CO_2 ≈ 9.5% vol (1750 rpm, 100 Nm, 40 L/min) CO_2 ≈ 7.5% vol
[65]	0–21% HES Manifold inj. Type 1	Four cylinders Max. power: 55 kW at 3900 rpm Max. torque: 156 Nm at 2000 rpm Turbocharged	(2000 rpm, 55% load, no H_2) CO_2 ≈ 7.2% vol (2000 rpm, 55% load, 7% HES) CO_2 ≈ 6.9% vol (2000 rpm, 55% load, 13% HES) CO_2 ≈ 6.6% vol (2000 rpm, 55% load, 21% HES) CO_2 ≈ 6.2% vol
[21]	7 L/min Manifold inj. Type 1	Single cylinder Max. power: 5.2 kW at 1500 rpm Max. torque: No data Naturally aspirated	(1500 rpm, 30% load, no H_2) CO_2 ≈ 2.6% vol (1500 rpm, 30% load, 7 L/min) CO_2 ≈ 2.4% vol (1500 rpm, 50% load, no H_2) CO_2 ≈ 4% vol (1500 rpm, 50% load, 7 L/min) CO_2 ≈ 3.9% vol (1500 rpm, 100% load, no H_2) CO_2 ≈ 7% vol (1500 rpm, 100% load, 7 L/min) CO_2 ≈ 6.9% vol
[23]	0–10% HES Manifold inj. Type 2	Single cylinder Max. power: 7.35 kW at 3600 rpm Max. torque: No data Naturally aspirated	(3600 rpm, 60% load, no H_2) CO_2 = 6.71% vol (3600 rpm, 60% load, 6% HES) CO_2 = 5.82% vol (3600 rpm, 60% load, 8% HES) CO_2 = 5.63% vol (3600 rpm, 60% load, 10% HES) CO_2 = 5.38% vol
[24]	0–34% HES Manifold inj. Type 1	Single cylinder Max. power: 7 kW at 4200 rpm Max. torque: No data Naturally aspirated	(1500 rpm, 100% load, no H_2) CO_2 = 7.80% vol (1500 rpm, 100% load, 4% HES) CO_2 = 7.17% vol (1500 rpm, 100% load, 7% HES) CO_2 = 6.98% vol (1500 rpm, 100% load, 12% HES) CO_2 = 6.47% vol (1500 rpm, 100% load, 23% HES) CO_2 = 6.29% vol (1500 rpm, 100% load, 34% HES) CO_2 = 4.61% vol
[54]	0–30% HES Manifold inj. Type 1	Single cylinder Max. power: 5.2 kW at 1500 rpm Max. torque: No data Naturally aspirated	(1500 rpm, 25% load, no H_2) CO_2 ≈ 1700 g/kWh (1500 rpm, 25% load, 10% HES) CO_2 ≈ 1400 g/kWh (1500 rpm, 25% load, 30% HES) CO_2 ≈ 1250 g/kWh (1500 rpm, 50% load, no H_2) CO_2 ≈ 1100 g/kWh (1500 rpm, 50% load, 10% HES) CO_2 ≈ 950 g/kWh (1500 rpm, 50% load, 30% HES) CO_2 ≈ 800 g/kWh (1500 rpm, 100% load, no H_2) CO_2 ≈ 850 g/kWh (1500 rpm, 100% load, 10% HES) CO_2 ≈ 750 g/kWh (1500 rpm, 100% load, 30% HES) CO_2 ≈ 550 g/kWh
[22]	0–0.08 kg/h (0–28% HES) Port inj. Type 2	Single cylinder Max. power: 7.4 kW at 3600 rpm Max. torque: 28 Nm at 2000 rpm Naturally aspirated	(1800 rpm, 10 Nm, no H_2) CO_2 ≈ 690 g/kWh (1800 rpm, 10 Nm, 7.5% HES) CO_2 ≈ 675 g/kWh (1800 rpm, 10 Nm, 17.5% HES) CO_2 ≈ 650 g/kWh (1800 rpm, 10 Nm, 28% HES) CO_2 ≈ 620 g/kWh
[55]	0–20% HES Manifold inj. Type 1	Single cylinder Max. power: 5.2 kW at 1500 rpm Max. torque: No data Naturally aspirated	(1500 rpm, 25% load, no H_2) CO_2 ≈ 37,000 ppm (1500 rpm, 25% load, 20% HES) CO_2 ≈ 32,000 ppm (1500 rpm, 50% load, no H_2) CO_2 ≈ 52,000 ppm (1500 rpm, 50% load, 20% HES) CO_2 ≈ 43,000 ppm (1500 rpm, 75% load, no H_2) CO_2 ≈ 65,000 ppm (1500 rpm, 75% load, 20% HES) CO_2 ≈ 56,000 ppm
[56]	0–36 L/min (0–86% HES) Manifold inj. Type 2	Single cylinder Max. power: 5.97 kW at 2200 rpm Max. torque: No data	(1850 rpm, 12 Nm load, no H_2) CO_2 ≈ 5% vol (1850 rpm, 12 Nm load, 12 L/min) CO_2 ≈ 4.5% vol (1850 rpm, 12 Nm load, 24 L/min) CO_2 ≈ 2.5% vol (1850 rpm, 12 Nm load, 36 L/min) CO_2 ≈ 2.25% vol (1850 rpm, 20 Nm load, no H_2) CO_2 ≈ 7.5% vol (1850 rpm, 20 Nm load, 12 L/min) CO_2 ≈ 7% vol (1850 rpm, 20 Nm load, 24 L/min) CO_2 ≈ 6% vol (1850 rpm, 20 Nm load, 36 L/min) CO_2 ≈ 5% vol

Table 8. *Cont.*

Ref.	H_2 Enrichment and Mixing Process Type of Test	Engine Specifications	Key Findings (CO_2=) Data Directly Reflected in the Document (CO_2≈) Approximately Measured Data in the Document's Figures
[64]	0–50% HES Manifold inj. Type 2	Single cylinder Max. power: 13.2 kW at 1500 rpm Max. torque: No data Naturally aspirated	(965 rpm, ML, no H_2) $CO_2 \approx 4.6\%$ vol (965 rpm, ML, 15% HES) $CO_2 \approx 4.4\%$ vol (965 rpm, ML, 41% HES) $CO_2 \approx 3.4\%$ vol (965 rpm, NL, no H_2) $CO_2 \approx 6.9\%$ vol (965 rpm, NL, 14% HES) $CO_2 \approx 6.7\%$ vol (965 rpm, NL, 33% HES) $CO_2 \approx 5.7\%$ vol

HES: hydrogen energy share, ML: medium load, NL: nominal load.

All consulted authors, irrespective of engine size, have observed an identical trend: a rise in CO_2 emissions with an increase in engine load and a decrease with growing HES. The majority of authors state that using H_2, a carbon-free fuel, instead of diesel fuel helps in reducing emissions. In a study by Castro et al. [36] concerning a four-cylinder engine, the decrease in CO_2 emissions matched the reduction in diesel fuel consumption. For example, at a 60% HES level, the reduction in CO_2 was 45.7%, while the decrease in diesel fuel consumption was 43.9%. Comparable findings were presented in the studies by Cernat et al. [65] and Subramanian and Thangavel [56]. Additionally, Rocha et al. [23] established a correlation between CO_2, CO, HC, and PM, contending that a reduction in the levels of the latter three (which will be discussed below) results in an increase in CO_2 emissions. The study found that the decrease in CO_2 emissions was less than the decrease in carbon provided by diesel fuel, suggesting that a higher amount of carbon from CO, HC, and PM was converted to CO_2.

2.2.2. CO Emissions

CO is a colorless and odorless gas resulting from incomplete combustion of carbon-based fuels. In CIEs, where the fuel–air mixture is usually lean, CO oxidation to CO_2 is insufficient due to inadequate mixing of the fuel before ignition, leading to the presence of fuel-rich and fuel-lean areas [24,69,70]. The lack of sufficient O_2 in the fuel-rich area prevents complete oxidation to form CO_2. In fuel-lean conditions, incomplete oxidation occurs due to lower temperatures and combustion rates. This particular compound can be oxidized in the atmosphere to form CO_2 through a reversible chemical reaction (Equation (4) [71]) and may be indirectly classified as a GHG. Table 9 displays recent notable studies that investigate CO emissions in the presence of H_2.

$$2\,CO + O_2 \leftrightarrow 2\,CO_2 + 173\ kJ\ mol^{-1}. \quad (4)$$

Table 9. Results of CO emissions with the addition of H_2.

Ref.	H_2 Enrichment and Mixing Process Type of Test	Engine Specifications	Key Findings (CO=) Data Directly Reflected in the Document (CO≈) Approximately Measured Data in the Document's Figures
[50]	25 L/min Carburetor Type 2	Four cylinders Max. power: 60 kW at 2200 rpm Max. torque: No data Naturally aspirated	(2200 rpm, 25% load, no H_2) $CO \approx 0.24\%$ vol (2200 rpm, 25% load, 25 L/min) $CO \approx 0.06\%$ vol (2200 rpm, 50% load, no H_2) $CO \approx 0.26\%$ vol (2200 rpm, 50% load, 25 L/min) $CO \approx 0.09\%$ vol (2200 rpm, 100% load, no H_2) $CO \approx 0.85\%$ vol (2200 rpm, 100% load, 25 L/min) $CO \approx 0.41\%$ vol

Table 9. *Cont.*

Ref.	H_2 Enrichment and Mixing Process Type of Test	Engine Specifications	Key Findings (CO=) Data Directly Reflected in the Document (CO≈) Approximately Measured Data in the Document's Figures
[52]	0–30% HES Direct inj. Type 1	Two cylinders Max. power: 21 kW at 2200 rpm Max. torque: No data Naturally aspirated	(50% load, no H_2) CO ≈ 2.8 g/kWh (50% load, 10% HES) CO ≈ 2.6 g/kWh (50% load, 20% HES) CO ≈ 2.4 g/kWh (50% load, 30% HES) CO ≈ 1.7 g/kWh (100% load, no H_2) CO ≈ 4.2 g/kWh (100% load, 10% HES) CO ≈ 3.7 g/kWh (100% load, 20% HES) CO ≈ 3.6 g/kWh (100% load, 30% HES) CO ≈ 3 g/kWh
[21]	7 L/min Manifold inj. Type 1	Single cylinder Max. power: 5.2 kW at 1500 rpm Max. torque: No data Naturally aspirated	(1500 rpm, 30% load, no H_2) CO ≈ 0.085% vol (1500 rpm, 30% load, 7 L/min) CO ≈ 0.082% vol (1500 rpm, 50% load, no H_2) CO ≈ 0.08% vol (1500 rpm, 50% load, 7 L/min) CO ≈ 0.07% vol (1500 rpm, 100% load, no H_2) CO ≈ 0.14% vol (1500 rpm, 100% load, 7 L/min) CO ≈ 0.12% vol
[23]	0–10% HES Manifold inj. Type 2	Single cylinder Max. power: 7.35 kW at 3600 rpm Max. torque: No data Naturally aspirated	(3600 rpm, 60% load, no H_2) CO = 1850.3 ppm (3600 rpm, 60% load, 2% HES) CO = 1137.2 ppm (3600 rpm, 60% load, 6% HES) CO = 801.6 ppm (3600 rpm, 60% load, 8% HES) CO = 751.5 ppm (3600 rpm, 60% load, 10% HES) CO = 676.4 ppm
[24]	0–34% HES Manifold inj. Type 1	Single cylinder Max. power: 7 kW at 4200 rpm Max. torque: No data Naturally aspirated	(1500 rpm, 100% load, no H_2) CO = 7.80% vol (1500 rpm, 100% load, 4% HES) CO = 7.17% vol (1500 rpm, 100% load, 7% HES) CO = 6.98% vol (1500 rpm, 100% load, 12% HES) CO = 6.47% vol (1500 rpm, 100% load, 23% HES) CO = 6.29% vol (1500 rpm, 100% load, 34% HES) CO = 4.61% vol
[54]	0–30% HES Manifold inj. Type 1	Single cylinder Max. power: 5.2 kW at 1500 rpm Max. torque: No data Naturally aspirated	(1500 rpm, 25% load, no H_2) CO ≈ 37 g/kWh (1500 rpm, 25% load, 10% HES) CO ≈ 27 g/kWh (1500 rpm, 25% load, 30% HES) CO ≈ 20 g/kWh (1500 rpm, 50% load, no H_2) CO ≈ 16 g/kWh (1500 rpm, 50% load, 10% HES) CO ≈ 13 g/kWh (1500 rpm, 50% load, 30% HES) CO ≈ 10 g/kWh (1500 rpm, 100% load, no H_2) CO ≈ 9 g/kWh (1500 rpm, 100% load, 10% HES) CO ≈ 8 g/kWh (1500 rpm, 100% load, 30% HES) CO ≈ 5 g/kWh
[22]	0–0.08 kg/h (0–28% HES) Port inj. Type 2	Single cylinder Max. power: 7.4 kW at 3600 rpm Max. torque: 28 Nm at 2000 rpm Naturally aspirated	(1800 rpm, 10 Nm, no H_2) CO ≈ 14 g/kWh (1800 rpm, 10 Nm, 7.5% HES) CO ≈ 12.7 g/kWh (1800 rpm, 10 Nm, 17.5% HES) CO ≈ 11 g/kWh (1800 rpm, 10 Nm, 28% HES) CO ≈ 8 g/kWh
[55]	0–20% HES Manifold inj. Type 1	Single cylinder Max. power: 5.2 kW at 1500 rpm Max. torque: No data Naturally aspirated	1500 rpm, 25% load, no H_2) CO ≈ 590 ppm (1500 rpm, 25% load, 20% HES) CO ≈ 550 ppm (1500 rpm, 50% load, no H_2) CO ≈ 340 ppm (1500 rpm, 50% load, 20% HES) CO ≈ 300 ppm (1500 rpm, 75% load, no H_2) CO ≈ 270 ppm (1500 rpm, 75% load, 20% HES) CO ≈ 210 ppm
[64]	0–50% HES Manifold inj. Type 2	Single cylinder Max. power: 13.2 kW at 1500 rpm Max. torque: No data Naturally aspirated	(965 rpm, ML, no H_2) CO ≈ 1500 ppm (965 rpm, ML, 15% HES) CO ≈ 1200 ppm (965 rpm, ML, 41% HES) CO ≈ 800 ppm (965 rpm, NL, no H_2) CO ≈ 2800 ppm (965 rpm, NL, 14% HES) CO ≈ 3200 ppm (965 rpm, NL, 33% HES) CO ≈ 2800 ppm
[66]	0–15 L/min Manifold inj. Type 2	Single cylinder Max. power: 5.2 kW at 1500 rpm Max. torque: No data Naturally aspirated	(1500 rpm, 0% load, no H_2) CO ≈ 14 g/kWh (1500 rpm, 0% load, 15 L/min) CO = 9.89 g/kWh (1500 rpm, 100% load, no H_2) CO = 59.95 g/kWh (1500 rpm, 100% load, 15 L/min) CO = 52.97 g/kWh

HES: hydrogen energy share, ML: medium load, NL: nominal load.

For commercial engines intended for use in conventional vehicles, it has been found that increasing loads lead to a rise in CO emissions. Although most authors agree, Sharma et al. [55] noted a decrease in these emissions with increased loads. Their argument was

that in-cylinder temperature rises, which can hasten CO oxidation to CO_2. Similarly to CO_2, all authors point out that the lack of carbon atoms in hydrogen results in a decrease in CO emissions, despite differences in loading. Nag et al. [54] found that at 1500 rpm and 25% load, 10% and 30% HES resulted in a 29.1% and 46.8% decrease in CO emissions, respectively. Moreover, Rocha et al. [23] reported that the maximum reduction in diesel fuel consumption was 15.8% (10% HES), whereas CO reduction was 63.4%. This indicates a faster combustion reaction. Nevertheless, there is a divergence in this trend when it comes to single-cylinder engines.

2.2.3. Hydrocarbons

HC emissions are organic compounds with a bluish color and a pungent odor that typically result from incomplete diesel fuel combustion. In situations of low loads, fuel does not completely ignite due to a lean fuel–air mixture. Additionally, over-fueling can contribute to HC emissions, as there are areas in the combustion chamber with an over-rich fuel–air mixture, resulting in incomplete combustion. Table 10 displays some of the most significant recent studies examining HC emissions with the inclusion of H_2.

Table 10. Results of HC emissions with the addition of H_2.

Ref.	H_2 Enrichment and Mixing Process Type of Test	Engine Specifications	Key Findings (HC=) Data Directly Reflected in the Document (HC≈) Approximately Measured Data in the Document's Figures
[49]	0–25% HES Manifold inj. Type 1	Four cylinders Max. power: 103 kW at 4000 rpm Max. torque: 320 Nm at 1750–2500 rpm Turbocharged	(2000 rpm, 15% load, no H_2) HC = 21.20 ppm (2000 rpm, 15% load, 25% HES) HC = 16.89 ppm (2000 rpm, 30% load, no H_2) HC = 15.07 ppm (2000 rpm, 30% load, 25% HES) HC = 9.92 ppm (2000 rpm, 45% load, no H_2) HC = 8.39 ppm (2000 rpm, 45% load, 25% HES) HC = 5.17 ppm
[50]	25 L/min Carburetor Type 2	Four cylinders Max. power: 60 kW at 2200 rpm Max. torque: No data Naturally aspirated	(2200 rpm, 25% load, no H_2) HC ≈ 185 ppm (2200 rpm, 25% load, 25 L/min) HC ≈ 100 ppm (2200 rpm, 50% load, no H_2) HC ≈ 200 ppm (2200 rpm, 50% load, 25 L/min) HC ≈ 105 ppm (2200 rpm, 100% load, no H_2) HC ≈ 345 ppm (2200 rpm, 100% load, 25 L/min) HC ≈ 110 ppm
[51]	0–40 L/min Carburetor Type 2	Four cylinders Max. power: 48 kW at 4000 rpm Max. torque: 160 Nm at 1750 rpm Turbocharged	1750 rpm, 50 Nm, no H_2) HC ≈ 41 ppm (1750 rpm, 50 Nm, 20 L/min) HC ≈ 30 ppm (1750 rpm, 50 Nm, 40 L/min) HC ≈ 33 ppm (1750 rpm, 75 Nm, no H_2) HC ≈ 39 ppm (1750 rpm, 75 Nm, 20 L/min) HC ≈ 32 ppm (1750 rpm, 75 Nm, 40 L/min) HC ≈ 36 ppm (1750 rpm, 100 Nm, no H_2) HC ≈ 40 ppm (1750 rpm, 100 Nm, 20 L/min) HC ≈ 35 ppm (1750 rpm, 100 Nm, 40 L/min) HC ≈ 37 ppm
[52]	0–30% HES Direct inj. Type 1	Two cylinders Max. power: 21 kW at 2200 rpm Max. torque: No data Naturally aspirated	(50% load, no H_2) HC ≈ 0.37 g/kWh (50% load, 10% HES) HC ≈ 0.30 g/kWh (50% load, 20% HES) HC ≈ 0.28 g/kWh (50% load, 30% HES) HC ≈ 0.25 g/kWh (100% load, no H_2) HC ≈ 0.39 g/kWh (100% load, 10% HES) HC = 0.37 g/kWh (100% load, 20% HES) HC = 0.32 g/kWh (100% load, 30% HES) HC = 0.28 g/kWh
[65]	0–21% HES Manifold inj. Type 1	Four cylinders Max. power: 55 kW at 3900 rpm Max. torque: 156 Nm at 2000 rpm Turbocharged	(2000 rpm, 55% load, no H_2) HC ≈ 7 ppm (2000 rpm, 55% load, 7% HES) HC ≈ 6 ppm (2000 rpm, 55% load, 13% HES) HC ≈ 5 ppm (2000 rpm, 55% load, 21% HES) HC ≈ 5 ppm
[21]	7 L/min Manifold inj. Type 1	Single cylinder Max. power: 5.2 kW at 1500 rpm Max. torque: No data Naturally aspirated	(1500 rpm, 30% load, no H_2) HC ≈ 18 ppm (1500 rpm, 30% load, 7 L/min) HC ≈ 17 ppm (1500 rpm, 50% load, no H_2) HC ≈ 27 ppm (1500 rpm, 50% load, 7 L/min) HC ≈ 24 ppm (1500 rpm, 100% load, no H_2) HC ≈ 46 ppm (1500 rpm, 100% load, 7 L/min) HC ≈ 45 ppm

Table 10. *Cont.*

Ref.	H_2 Enrichment and Mixing Process Type of Test	Engine Specifications	Key Findings (HC=) Data Directly Reflected in the Document (HC≈) Approximately Measured Data in the Document's Figures
[23]	0–10% HES Manifold inj. Type 2	Single cylinder Max. power: 7.35 kW at 3600 rpm Max. torque: No data Naturally aspirated	(3600 rpm, 60% load, no H_2) HC = 435.4 ppm (3600 rpm, 60% load, 2% HES) HC = 258.4 ppm (3600 rpm, 60% load, 6% HES) HC = 142.2 ppm (3600 rpm, 60% load, 8% HES) HC = 59.9 ppm (3600 rpm, 60% load, 10% HES) HC = 9 ppm
[24]	0–34% HES Manifold inj. Type 1	Single cylinder Max. power: 7 kW at 4200 rpm Max. torque: No data Naturally aspirated	(1500 rpm, 100% load, no H_2) HC = 81 ppm (1500 rpm, 100% load, 4% HES) HC = 86 ppm (1500 rpm, 100% load, 7% HES) HC = 89 ppm (1500 rpm, 100% load, 12% HES) HC = 96 ppm (1500 rpm, 100% load, 23% HES) HC = 88 ppm (1500 rpm, 100% load, 34% HES) HC = 87 ppm
[54]	0–30% HES Manifold inj. Type 1	Single cylinder Max. power: 5.2 kW at 1500 rpm Max. torque: No data Naturally aspirated	(1500 rpm, 25% load, no H_2) HC ≈ 65 g/kWh (1500 rpm, 25% load, 10% HES) HC ≈ 62 g/kWh (1500 rpm, 25% load, 30% HES) HC ≈ 60 g/kWh (1500 rpm, 50% load, no H_2) HC ≈ 38 g/kWh (1500 rpm, 50% load, 10% HES) HC ≈ 35 g/kWh (1500 rpm, 50% load, 30% HES) HC ≈ 32 g/kWh (1500 rpm, 100% load, no H_2) HC ≈ 29 g/kWh (1500 rpm, 100% load, 10% HES) HC ≈ 23 g/kWh (1500 rpm, 100% load, 30% HES) HC ≈ 20 g/kWh
[22]	0–0.08 kg/h (0–28% HES) Port inj. Type 2	Single cylinder Max. power: 7.4 kW at 3600 rpm Max. torque: 28 Nm at 2000 rpm Naturally aspirated	(1800 rpm, 10 Nm, no H_2) HC ≈ 0.13 g/kWh (1800 rpm, 10 Nm, 7.5% HES) HC ≈ 0.13 g/kWh (1800 rpm, 10 Nm, 17.5% HES) HC ≈ 0.12 g/kWh (1800 rpm, 10 Nm, 28% HES) HC ≈ 0.10 g/kWh
[55]	0–20% HES Manifold inj. Type 1	Single cylinder Max. power: 5.2 kW at 1500 rpm Max. torque: No data Naturally aspirated	(1500 rpm, 25% load, no H_2) HC = 381 ppm (1500 rpm, 25% load, 20% HES) HC = 399.6 ppm (1500 rpm, 50% load, no H_2) HC = 456.06 ppm (1500 rpm, 50% load, 20% HES) HC = 436.58 ppm (1500 rpm, 75% load, no H_2) HC = 446.32 ppm (1500 rpm, 75% load, 20% HES) HC = 419.85 ppm
[56]	0–36 L/min (0–86% HES) Manifold inj. Type 2	Single cylinder Max. power: 5.97 kW at 2200 rpm Max. torque: No data	(1850 rpm, 12 Nm load, no H_2) HC ≈ 30 ppm (1850 rpm, 12 Nm load, 12 L/min) HC ≈ 55 ppm (1850 rpm, 12 Nm load, 24 L/min) HC ≈ 60 ppm (1850 rpm, 12 Nm load, 36 L/min) HC ≈ 80 ppm (1850 rpm, 20 Nm load, no H_2) HC ≈ 70 ppm (1850 rpm, 20 Nm load, 12 L/min) HC ≈ 100 ppm (1850 rpm, 20 Nm load, 24 L/min) HC ≈ 135 ppm (1850 rpm, 20 Nm load, 36 L/min) HC ≈ 125 ppm
[64]	0–50% HES Manifold inj. Type 2	Single cylinder Max. power: 13.2 kW at 1500 rpm Max. torque: No data Naturally aspirated	(965 rpm, ML, no H_2) HC ≈ 85 ppm (965 rpm, ML, 15% HES) HC ≈ 90 ppm (965 rpm, ML, 41% HES) HC ≈ 80 ppm (965 rpm, NL, no H_2) HC ≈ 95 ppm (965 rpm, NL, 14% HES) HC ≈ 105 ppm (965 rpm, NL, 33% HES) HC ≈ 95 ppm

HES: hydrogen energy share, ML: medium load, NL: nominal load.

For commercial vehicle engines, it has been found that the use of H_2 results in a reduction in HC emissions. This decline is due to the lack of carbon atoms in hydrogen, as previously mentioned. The majority of studies note a trend towards a greater reduction of HC emissions with an increase in the quantity of hydrogen. This correlation also holds true for CO_2 and CO. However, Yilmaz and Gumus [51] reported higher HC emissions for a hydrogen supply of 40 L/min compared to 20 L/min. They argued that the increase may be attributed to a lack of oxygen during diffusion combustion, as the instantaneous combustion of hydrogen consumes most of the available oxygen. This trend was further confirmed for BTE.

Most studies indicate a downward trend for lower-powered engines. Kanth et al. [21] and Rocha et al. [23] explained that hydrogen's higher flame speed leads to better combustion efficiency, resulting in HC reduction. However, contradictory results were observed by Sharma and Dhar [55], who reported increasing HC emissions for lower HES concentrations. They

stated that very low levels of HES affected the competition between OH and H radicals during the high-temperature phase of combustion. Subramanian and Thangavel [56] hypothesized that higher HC emissions for lower HES may be attributed to decreased air excess and lower combustion temperature, which increase the likelihood of incomplete combustion. Tutak et al.'s research [24] demonstrated that HC emissions displayed an upward trend with supplementation below 12% HES and decreased with higher HES supplementations. Nonetheless, emissions stayed below 100 ppm, an amount considered negligible. It is worth mentioning that the study denotes an equipment measuring accuracy of ±12 ppm.

2.2.4. Soot/PM/Smoke

Soot formation in CIEs is attributed to the presence of heterogeneous mixtures of air and fuel. The degree of homogeneity of the mixture can be increased to significantly reduce soot emissions. Soot formation typically occurs in areas with oxygen defects in the combustion chamber, where fuel oxidation is not allowed [39]. Lubricating oils can also be a contributing factor to soot emissions [72]. Table 11 presents some of the recent studies exploring soot emissions with the incorporation of H_2.

Table 11. Results of soot emissions with the addition of H_2.

Ref.	H_2 Enrichment and Mixing Process Type of Test	Engine Specifications	Key Findings (PM=) Data Directly Reflected in the Document (PM≈) Approximately Measured Data in the Document's Figures
[49]	0–25% HES Manifold inj. Type 1	Four cylinders Max. power: 103 kW at 4000 rpm Max. torque: 320 Nm at 1750–2500 rpm Turbocharged	(2000 rpm, 15% load, no H_2) PM = 7.12×10^7 #/cc (2000 rpm, 15% load, 25% HES) PM = 4.75×10^7 #/cc (2000 rpm, 30% load, no H_2) PM = 1.00×10^8 #/cc (2000 rpm, 30% load, 25% HES) PM = 8.48×10^7 #/cc (2000 rpm, 45% load, no H_2) PM = 1.43×10^8 #/cc (2000 rpm, 45% load, 25% HES) PM = 9.39×10^7 #/cc
[36]	0–80% HES Manifold inj. Type 1	Four cylinders Max. power: 58 kW at 4500 rpm Max. torque: 145 Nm at 2350 rpm Turbocharged	(2400 rpm, 30% load, no H_2) K ≈ 0.20 m^{-1} (2400 rpm, 30% load, 30% HES) K ≈ 0.05 m^{-1} (2400 rpm, 30% load, 80% HES) K ≈ 0.05 m^{-1} (2400 rpm, 60% load, no H_2) K ≈ 0.22 m^{-1} (2400 rpm, 60% load, 30% HES) K ≈ 0.21 m^{-1} (2400 rpm, 60% load, 60% HES) K ≈ 0.17 m^{-1} (2400 rpm, 100% load, no H_2) K ≈ 0.97 m^{-1} (2400 rpm, 100% load, 30% HES) K ≈ 0.55 m^{-1} (2400 rpm, 100% load, 40% HES) K ≈ 0.95 m^{-1}
[65]	0–21% HES Manifold inj. Type 1	Four cylinders Max. power: 55 kW at 3900 rpm Max. torque: 156 Nm at 2000 rpm Turbocharged	(2000 rpm, 55% load, no H_2) K ≈ 2.1 m^{-1} (2000 rpm, 55% load, 7% HES) K ≈ 1.6 m^{-1} (2000 rpm, 55% load, 13% HES) K ≈ 1.7 m^{-1} (2000 rpm, 55% load, 21% HES) K ≈ 1.8 m^{-1}
[21]	7 L/min Manifold inj. Type 1	Single cylinder Max. power: 5.2 kW at 1500 rpm Max. torque: No data Naturally aspirated	(1500 rpm, 30% load, no H_2) HC ≈ 18 ppm (1500 rpm, 30% load, 7 L/min) HC ≈ 17 ppm (1500 rpm, 50% load, no H_2) HC ≈ 27 ppm (1500 rpm, 50% load, 7 L/min) HC ≈ 24 ppm (1500 rpm, 100% load, no H_2) HC ≈ 46 ppm (1500 rpm, 100% load, 7 L/min) HC ≈ 45 ppm
[24]	0–34% HES Manifold inj. Type 1	Single cylinder Max. power: 7 kW at 4200 rpm Max. torque: No data Naturally aspirated	(1500 rpm, 100% load, no H_2) smoke ≈ 863 mg/m^3 (1500 rpm, 100% load, 4% HES) smoke ≈ 640 mg/m^3 (1500 rpm, 100% load, 7% HES) smoke ≈ 336 mg/m^3 (1500 rpm, 100% load, 12% HES) smoke ≈ 203 mg/m^3 (1500 rpm, 100% load, 23% HES) smoke ≈ 134 mg/m^3 (1500 rpm, 100% load, 34% HES) smoke ≈ 143 mg/m^3
[54]	0–30% HES Manifold inj. Type 1	Single cylinder Max. power: 5.2 kW at 1500 rpm Max. torque: No data Naturally aspirated	(1500 rpm, 25% load, no H_2) PM ≈ 5.00×10^7 #/cc (1500 rpm, 25% load, 10% HES) PM ≈ 4.50×10^7 #/cc (1500 rpm, 25% load, 30% HES) PM ≈ 4.00×10^7 #/cc (1500 rpm, 50% load, no H_2) PM ≈ 3.50×10^7 #/cc (1500 rpm, 50% load, 10% HES) PM ≈ 3.50×10^7 #/cc (1500 rpm, 50% load, 30% HES) PM ≈ 2.90×10^7 #/cc (1500 rpm, 100% load, no H_2) PM ≈ 5.60×10^7 #/cc (1500 rpm, 100% load, 10% HES) PM ≈ 5.00×10^7 #/cc (1500 rpm, 100% load, 30% HES) PM ≈ 3.50×10^7 #/cc
[22]	0–0.08 kg/h (0–28% HES) Port inj. Type 2	Single cylinder Max. power: 7.4 kW at 3600 rpm Max. torque: 28 Nm at 2000 rpm Naturally aspirated	(1800 rpm, 10 Nm, no H_2) PM = 18.64 g/kWh (1800 rpm, 10 Nm, 7.5% HES) PM ≈ 14.5 g/kWh (1800 rpm, 10 Nm, 17.5% HES) PM ≈ 12.0 g/kWh (1800 rpm, 10 Nm, 28% HES) PM = 5.95 g/kWh

Table 11. *Cont.*

Ref.	H_2 Enrichment and Mixing Process Type of Test	Engine Specifications	Key Findings (PM=) Data Directly Reflected in the Document (PM≈) Approximately Measured Data in the Document's Figures
[55]	0–20% HES Manifold inj. Type 1	Single cylinder Max. power: 5.2 kW at 1500 rpm Max. torque: No data Naturally aspirated	(1500 rpm, 25% load, no H_2) PM ≈ 1.6×10^7 #/cc (1500 rpm, 25% load, 20% HES) PM ≈ 1.3×10^7 #/cc (1500 rpm, 50% load, no H_2) PM ≈ 4.8×10^7 #/cc (1500 rpm, 50% load, 20% HES) PM ≈ 3.7×10^7 #/cc (1500 rpm, 75% load, no H_2) PM ≈ 5.3×10^7 #/cc (1500 rpm, 75% load, 20% HES) PM ≈ 4.1×10^7 #/cc
[56]	0–36 L/min (0–86% HES) Manifold inj. Type 2	Single cylinder Max. power: 5.97 kW at 2200 rpm Max. torque: No data	(1850 rpm, 12 Nm load, no H_2) smoke ≈ 62% vol (1850 rpm, 12 Nm load, 12 L/min) smoke ≈ 50% vol (1850 rpm, 12 Nm load, 24 L/min) smoke ≈ 32% vol (1850 rpm, 12 Nm load, 36 L/min) smoke ≈ 19% vol (1850 rpm, 20 Nm load, no H_2) smoke ≈ 70% vol (1850 rpm, 20 Nm load, 12 L/min) smoke ≈ 78% vol (1850 rpm, 20 Nm load, 24 L/min) smoke ≈ 60% vol (1850 rpm, 20 Nm load, 36 L/min) smoke ≈ 48% vol
[64]	0–50% HES Manifold inj. Type 2	Single cylinder Max. power: 13.2 kW at 1500 rpm Max. torque: No data Naturally aspirated	(965 rpm, ML, no H_2) smoke ≈ 24% vol (965 rpm, ML, 15% HES) smoke ≈ 18% vol (965 rpm, ML, 41% HES) smoke ≈ 13% vol (965 rpm, NL, no H_2) smoke ≈ 21% vol (965 rpm, NL, 14% HES) smoke ≈ 14% vol (965 rpm, NL, 33% HES) smoke ≈ 6% vol

HES: hydrogen energy share, ML: medium load, NL: nominal load, K: opacity, PM: particulate matter, #/cc: particulate number density.

All consulted authors, regardless of engine size, demonstrated a consistent pattern: an increase in soot/PM with increasing load and a decrease with increasing HES. Most authors reported that hydrogen's high diffusivity facilitates the formation of a more uniform mixture, consequently providing fewer locations where pilot fuel cannot oxidize. In addition, they advocate for swapping fossil fuels with carbon-free alternatives, such as hydrogen.

2.2.5. NO_x Emissions

NO_x refers to gaseous binary chemical compounds that form when nitrogen and oxygen combine. Emissions of NO_x from exhaust primarily contain NO and NO_2 in a 95-5 ratio, respectively [73]. N_2 and O_2 do not react at normal temperature and pressure (NTP), but reaction occurs in the combustion chamber under the necessary conditions. In an ICE, three mechanisms contribute to NO_x formation, namely, thermal NO_x, prompt NO_x, and fuel NO_x [74]. The Zeldovich mechanism is the principal NO_x formation route, brought about by the high combustion chamber temperature, where N_2 from the air is oxidized (described by Equation (5)) [23,25]. The Arrhenius law [75,76] confirms that NO formation rises exponentially with temperature. This chemical reaction strongly relies on the local combustion temperature, which is influenced by fuel–air distribution, O_2 concentration, pressure, and temperature of the intake charge, as well as the effective combustion volume [77]. Table 12 shows some of the most relevant recent studies in which soot emissions, with the addition of H_2, are studied.

$$N_2 + O_2 \rightarrow 2\,NO. \quad (5)$$

Table 12. Results of NO_x emissions with the addition of H_2.

Ref.	H_2 Enrichment and Mixing Process Type of Test	Engine Specifications	Key Findings (NO_x=) Data Directly Reflected in the Document (NO_x≈) Approximately Measured Data in the Document Figures
[49]	0–25% HES Manifold inj. Type 1	Four cylinders Max. power: 103 kW at 4000 rpm Max. torque: 320 Nm at 1750–2500 rpm Turbocharged	(2000 rpm, 15% load, no H_2) NO_x = 101.03 ppm (2000 rpm, 15% load, 25% HES) NO_x = 101.63 ppm (2000 rpm, 30% load, no H_2) NO_x = 156.74 ppm (2000 rpm, 30% load, 25% HES) NO_x = 134.13 ppm (2000 rpm, 45% load, no H_2) NO_x = 228.83 ppm (2000 rpm, 45% load, 25% HES) NO_x = 253.59 ppm

Table 12. *Cont.*

Ref.	H_2 Enrichment and Mixing Process Type of Test	Engine Specifications	Key Findings (NO_x=) Data Directly Reflected in the Document (NO_x≈) Approximately Measured Data in the Document Figures
[52]	0–30% HES Direct inj. Type 1	Two cylinders Max. power: 21 kW at 2200 rpm Max. torque: No data Naturally aspirated	(25% load, no H_2) NO_x = 6.1 g/kWh (25% load, 10% HES) NO_x = 6.3 g/kWh (25% load, 20% HES) NO_x = 6.6 g/kWh (25% load, 30% HES) NO_x = 7 g/kWh (50% load, no H_2) NO_x ≈ 6.5 g/kWh (50% load, 10% HES) NO_x ≈ 6.8 g/kWh (50% load, 20% HES) NO_x ≈ 7.1 g/kWh (50% load, 30% HES) NO_x ≈ 7.5 g/kWh (100% load, no H_2) NO_x ≈ 8.80 g/kWh (100% load, 10% HES) NO_x = 9.6 g/kWh (100% load, 20% HES) NO_x = 9.8 g/kWh (100% load, 30% HES) NO_x = 10.2 g/kWh
[65]	0–21% HES Manifold inj. Type 1	Four cylinders Max. power: 55 kW at 3900 rpm Max. torque: 156 Nm at 2000 rpm Turbocharged	(2000 rpm, 55% load, no H_2) NO_x ≈ 192 ppm (2000 rpm, 55% load, 7% HES) NO_x ≈ 150 ppm (2000 rpm, 55% load, 13% HES) NO_x ≈ 160 ppm (2000 rpm, 55% load, 21% HES) NO_x ≈ 185 ppm
[21]	7 L/min Manifold inj. Type 2	Single cylinder Max. power: 5.2 kW at 1500 rpm Max. torque: No data Naturally aspirated	(1500 rpm, 30% load, no H_2) NO_x ≈ 300 ppm (1500 rpm, 30% load, 7 L/min) NO_x ≈ 350 ppm (1500 rpm, 50% load, no H_2) NO_x ≈ 650 ppm (1500 rpm, 50% load, 7 L/min) NO_x ≈ 750 ppm (1500 rpm, 100% load, no H_2) NO_x ≈ 1400 ppm (1500 rpm, 100% load, 7 L/min) NO_x ≈ 1500 ppm
[23]	0–10% HES Manifold inj. Type 2	Single cylinder Max. power: 7.35 kW at 3600 rpm Max. torque: No data Naturally aspirated	(3600 rpm, 60% load, no H_2) NO_x = 182.4 ppm (3600 rpm, 60% load, 2% HES) NO_x = 221.25 ppm (3600 rpm, 60% load, 6% HES) NO_x = 224.38 ppm (3600 rpm, 60% load, 8% HES) NO_x = 236.93 ppm (3600 rpm, 60% load, 10% HES) NO_x = 270.50 ppm
[24]	0–34% HES Manifold inj. Type 1	Single cylinder Max. power: 7 kW at 4200 rpm Max. torque: No data Naturally aspirated	(1500 rpm, 100% load, no H_2) NO = 476 ppm (1500 rpm, 100% load, 4% HES) NO = 514 ppm (1500 rpm, 100% load, 7% HES) NO = 613 ppm (1500 rpm, 100% load, 12% HES) NO = 707 ppm (1500 rpm, 100% load, 23% HES) NO = 775 ppm (1500 rpm, 100% load, 34% HES) NO = 984 ppm
[37]	21.4–49.6 L/min Manifold inj. Type 2	Single cylinder Max. power: 10.3 kW at 3000 rpm Max. torque: 36 Nm at 2000 rpm Naturally aspirated	(2000 rpm, 5 Nm, 21.4 L/min) NO_x ≈ 400 ppm (2000 rpm, 5 Nm, 36.2 L/min) NO_x ≈ 220 ppm (2000 rpm, 5 Nm, 49.6 L/min) NO_x ≈ 70 ppm (2000 rpm, 15 Nm, 21.4 L/min) NO_x ≈ 750 ppm (2000 rpm, 15 Nm, 36.2 L/min) NO_x ≈ 750 ppm (2000 rpm, 15 Nm, 49.6 L/min) NO_x ≈ 750 ppm (2000 rpm, 20 Nm, 21.4 L/min) NO_x ≈ 880 ppm (2000 rpm, 20 Nm, 36.2 L/min) NO_x ≈ 900 ppm (2000 rpm, 20 Nm, 49.6 L/min) NO_x ≈ 1000 ppm
[54]	0–30% HES Manifold inj. Type 1	Single cylinder Max. power: 5.2 kW at 1500 rpm Max. torque: No data Naturally aspirated	(1500 rpm, 25% load, no H_2) NO_x ≈ 15 g/kWh (1500 rpm, 25% load, 10% HES) NO_x ≈ 14 g/kWh (1500 rpm, 25% load, 30% HES) NO_x ≈ 12 g/kWh (1500 rpm, 50% load, no H_2) NO_x ≈ 13.5 g/kWh (1500 rpm, 50% load, 10% HES) NO_x ≈ 13 g/kWh (1500 rpm, 50% load, 30% HES) NO_x ≈ 12.5 g/kWh (1500 rpm, 100% load, no H_2) NO_x ≈ 10.5 g/kWh (1500 rpm, 100% load, 10% HES) NO_x ≈ 10.5 g/kWh (1500 rpm, 100% load, 30% HES) NO_x ≈ 10 g/kWh
[22]	0–0.08 kg/h (0–28% HES) Port inj. Type 2	Single cylinder Max. power: 7.4 kW at 3600 rpm Max. torque: 28 Nm at 2000 rpm Naturally aspirated	(1800 rpm, 10 Nm, no H_2) NO_x ≈ 9.2 g/kWh (1800 rpm, 10 Nm, 7.5% HES) NO_x ≈ 9.8 g/kWh (1800 rpm, 10 Nm, 17.5% HES) NO_x ≈ 11.5 g/kWh (1800 rpm, 10 Nm, 28% HES) NO_x ≈ 15.5 g/kWh
[55]	0–20% HES Manifold inj. Type 1	Single cylinder Max. power: 5.2 kW at 1500 rpm Max. torque: No data Naturally aspirated	(1500 rpm, 25% load, no H_2) NO_x = 427.56 ppm (1500 rpm, 25% load, 20% HES) NO_x = 372.37 ppm (1500 rpm, 50% load, no H_2) NO_x = 746.31 ppm (1500 rpm, 50% load, 20% HES) NO_x = 661.52 ppm (1500 rpm, 75% load, no H_2) NO_x = 1016.3 ppm (1500 rpm, 75% load, 20% HES) NO_x = 1104.88 ppm

Table 12. *Cont.*

Ref.	H_2 Enrichment and Mixing Process Type of Test	Engine Specifications	Key Findings (NO_x=) Data Directly Reflected in the Document (NO_x≈) Approximately Measured Data in the Document Figures
[56]	0–36 L/min (0–86% HES) Manifold inj. Type 2	Single cylinder Max. power: 5.97 kW at 2200 rpm Max. torque: No data	(1850 rpm, 12 Nm load, no H_2) $NO_x \approx 200$ ppm (1850 rpm, 12 Nm load, 12 L/min) $NO_x \approx 100$ ppm (1850 rpm, 12 Nm load, 24 L/min) $NO_x \approx 120$ ppm (1850 rpm, 12 Nm load, 36 L/min) $NO_x \approx 100$ ppm (1850 rpm, 20 Nm load, no H_2) $NO_x \approx 450$ ppm (1850 rpm, 20 Nm load, 12 L/min) $NO_x \approx 410$ ppm (1850 rpm, 20 Nm load, 24 L/min) $NO_x \approx 520$ ppm (1850 rpm, 20 Nm load, 36 L/min) $NO_x \approx 600$ ppm

HES: Hydrogen energy share.

Studies on commercial engines for conventional vehicles do not yield conclusive results. Barrios et al.'s [49] work showed an unclear trend. NO_x emissions decreased with H_2 addition at a 30% load but increased at a 45% load. The authors argued that H_2 addition could lead to an increase in NO_x emissions due to a rise in gas temperature. However, in cases of low HES (25% in that study), this effect is mitigated as a result of exhaust gas mixture dilution from hydrogen-oxidation-induced water formation. Furthermore, it is worth noting that the EGR system was not controlled in that study, which could potentially affect combustion. At medium load, Cernat et al. [65] found a comparable pattern, showing a decrease in NO_x emissions with hydrogen substitution levels up to 7.5% HES. For higher HES levels, NO_x emissions rose, but they remained lower than those of diesel fuel. It is worth noting that H_2 substitution levels, as seen in the study by Barrios et al., remained relatively low, not exceeding 21% HES. However, Wu et al. [52] clearly found an increase in NO_x emissions with the addition of H_2, regardless of HES and engine load. This is due to the higher combustion rate of hydrogen compared to diesel fuel.

When discussing lower-powered engines, there are several important factors to consider. Sharma and Dhar [55], as well as Subramanian and Thangavel [56], supported previous findings of a slight decrease in NO_x emissions. They stated that it was due to a low level of H_2 substitution and its dilutive effect on oxygen displacement in the mixture at low and medium loads. However, both studies revealed an increase in NO_x emissions at higher loads, overall, with higher HES. Bakar et al. [37] presented a detailed overview of the impact of H_2 at various loads. They found that at low loads NO_x emissions were linked to the combustion zone of pilot diffusion, leading to very high temperatures and extended reaction times. The addition of H_2 reduced the quantity of pilot fuels, thus decreasing high-temperature combustion zones and resulting in a decline in NO_x emissions. At medium loads, NO_x emissions showed consistency. At high loads, the diesel fuel portion led to more efficient combustion. It increased in-cylinder pressure and, hence, NO_x emissions. However, other studies have indicated an increase in NO_x emissions independent of the load level and hydrogen substitution. This is argued to be due to the temperature increase in the combustion chamber.

3. Techniques for Emission Control and Enhancement of HES

The utilization of H_2 as an alternative fuel presents a potential solution to the reduction of pollutant emissions from CIEs, as discussed in the previous section. Nevertheless, its usage adversely affects NO_x emissions. As such, it is crucial to implement strategies to combat these emissions. Presented below are three feasible alternatives to decrease pollutant emissions associated with H_2 infusion, some of which are already implemented in traditional engines. These techniques, simultaneously, enable an increase in HES. In the following sections, both experimental and numerical studies, in which the model is validated with experimental data, have been considered.

3.1. Exhaust Gas Recirculation

The high temperatures attained in the combustion chamber cause reactions between atmospheric N_2 and other components, producing NO_x that is emitted into the atmosphere. To mitigate this, EGR is a highly precise system for reintroducing exhaust gases back into the intake manifold, thus modifying the incoming mixture's composition. This approach is widely utilized in contemporary CIEs. Studies investigating the advantages and disadvantages of this technology date back to the 1970s. According to the literature, the EGR rate refers to the alteration in air mass flow upon the introduction of EGR, and it can be computed using Equation (6).

$$EGR\ rate(\%) = \left(1 - \frac{\dot{m}_{air\ with\ EGR}}{\dot{m}_{air\ without\ EGR}}\right)100 \quad (6)$$

Table 13 presents notable recent studies that employed H_2 in conjunction with EGR to decrease NO_x emissions. The table specifies the EGR rate, the amount of H_2 utilized, and key outcomes of these investigations.

Table 13. Results of the reduction of NO_x with the addition of H_2 and EGR.

Ref.	H_2 Enrichment and Mixing Process Type of Test	Engine Specifications	Key Findings (NO_x=) Data Directly Reflected in the Document (NO_x≈) Approximately Measured Data in the Document's Figures
[50]	25 L/min Carburetor Type 2	Four cylinders Max. power: 60 kW at 2200 rpm Max. torque: No data Naturally aspirated	(2200 rpm, 100% load, no H_2, 0% EGR) NO_x = 535 ppm (2200 rpm, 100% load, 25 L/min, 0% EGR) NO_x = 590 ppm (2200 rpm, 100% load, 25 L/min, 10% EGR) NO_x = 504 ppm (2200 rpm, 100% load, 25 L/min, 20% EGR) NO_x = 463 ppm
[78]	0–41% HES Manifold inj. Type 1	Four cylinders Max. power: 85 kW at 4000 rpm Max. torque: No data Turbocharged	(1200 rpm, 8.5 bar MEP, 29% HES, 0% O_2 red.) $NO_x \approx$ 14 g/kWh (1200 rpm, 8.5 bar MEP, 29% HES, 1% O_2 red.) $NO_x \approx$ 13 g/kWh (1200 rpm, 8.5 bar MEP, 29% HES, 2% O_2 red.) $NO_x \approx$ 8 g/kWh (1200 rpm, 8.5 bar MEP, 29% HES, 3% O_2 red.) $NO_x \approx$ 4 g/kWh (1200 rpm, 11.5 bar MEP, 29% HES, 0% O_2 red.) $NO_x \approx$ 14 g/kWh (1200 rpm, 11.5 bar MEP, 29% HES, 1% O_2 red.) $NO_x \approx$ 10 g/kWh (1200 rpm, 11.5 bar MEP, 29% HES, 2% O_2 red.) $NO_x \approx$ 5 g/kWh (1200 rpm, 11.5 bar MEP, 29% HES, 3% O_2 red.) $NO_x \approx$ 2 g/kWh
[79]	0–8 L/min Manifold inj. Type 2	Four cylinders Max. power: 78.3 kW at 2500 rpm Max. torque: No data Turbocharged	(1500 rpm, 40% load, no H_2, 0% EGR) NO_x = 980 ppm (1500 rpm, 40% load, no H_2, 10% EGR) $NO_x \approx$ 300 ppm (1500 rpm, 40% load, no H_2, 20% EGR) $NO_x \approx$ 200 ppm (1500 rpm, 40% load, 4 L/min, 0% EGR) $NO_x \approx$ 1200 ppm (1500 rpm, 40% load, 4 L/min, 10% EGR) $NO_x \approx$ 400 ppm (1500 rpm, 40% load, 4 L/min, 20% EGR) $NO_x \approx$ 280 ppm (1500 rpm, 40% load, 8 L/min, 0% EGR) $NO_x \approx$ 1400 ppm (1500 rpm, 40% load, 8 L/min, 10% EGR) $NO_x \approx$ 440 ppm (1500 rpm, 40% load, 8 L/min, 20% EGR) NO_x = 283 ppm
[54]	0–30% HES Manifold inj. Type 1	Single cylinder Max. power: 5.2 kW at 1500 rpm Max. torque: No data Naturally aspirated	(1500 rpm, 100% load, no H_2) $NO_x \approx$ 10.5 g/kWh (1500 rpm, 100% load, 10% HES, 0% EGR) $NO_x \approx$ 10.5 g/kWh (1500 rpm, 100% load, 10% HES, 5% EGR) $NO_x \approx$ 7.5 g/kWh (1500 rpm, 100% load, 10% HES, 10% EGR) $NO_x \approx$ 6 g/kWh (1500 rpm, 100% load, 30% HES, 0% EGR) $NO_x \approx$ 10.5 g/kWh (1500 rpm, 100% load, 30% HES, 5% EGR) $NO_x \approx$ 8 g/kWh (1500 rpm, 100% load, 30% HES, 10% EGR) $NO_x \approx$ 7 g/kWh
[66]	0–15 L/min Manifold inj. Type 2	Single cylinder Max. power: 5.2 kW at 1500 rpm Max. torque: No data Naturally aspirated	(1500 rpm, 50% load, no H_2, 0% EGR) $NO_x \approx$ 12.5 g/kWh (1500 rpm, 50% load, 15 L/min, 0% EGR) $NO_x \approx$ 17.5 g/kWh (1500 rpm, 50% load, 15 L/min, 10% EGR) $NO_x \approx$ 14 g/kWh (1500 rpm, 100% load, no H_2, 0% EGR) NO_x = 9.5 g/kWh (1500 rpm, 100% load, 15 L/min, 0% EGR) NO_x = 12.9 g/kWh (1500 rpm, 100% load, 15 L/min, 10% EGR) NO_x = 10.49 g/kWh

Table 13. *Cont.*

Ref.	H_2 Enrichment and Mixing Process Type of Test	Engine Specifications	Key Findings (NO_x=) Data Directly Reflected in the Document (NO_x≈) Approximately Measured Data in the Document's Figures
[80]	2 L/min Manifold inj. Type 2	Single cylinder Max. power: 5.2 kW at 1500 rpm Max. torque: No data Naturally aspirated	(1500 rpm, 80% load, no H_2, 0% EGR) NO_x = 1300 ppm (1500 rpm, 80% load, 2 L/min, 0% EGR) NO_x = 1604 ppm (1500 rpm, 80% load, 2 L/min, 20% EGR) NO_x = 1150 ppm (1500 rpm, 100% load, no H_2, 0% EGR) NO_x ≈ 1100 ppm (1500 rpm, 100% load, 2 L/min, 0% EGR) NO_x ≈ 1500 ppm (1500 rpm, 100% load, 2 L/min, 20% EGR) NO_x ≈ 950 ppm
[81]	30 L/min Manifold inj. Type 2	Single cylinder Max. power: 5.2 kW at 1500 rpm Max. torque: No data Naturally aspirated	(1500 rpm, 25% load, no H_2, 0% EGR) NO_x ≈ 9.5 g/kWh (1500 rpm, 25% load, 30 L/min, 0% EGR) NO_x ≈ 13 g/kWh (1500 rpm, 25% load, 30 L/min, 30% EGR) NO_x ≈ 9.8 g/kWh (1500 rpm, 50% load, no H_2, 0% EGR) NO_x ≈ 6.8 g/kWh (1500 rpm, 50% load, 30 L/min, 0% EGR) NO_x ≈ 10 g/kWh (1500 rpm, 50% load, 30 L/min, 30% EGR) NO_x ≈ 7 g/kWh (1500 rpm, 100% load, no H_2, 0% EGR) NO_x = 5.09 g/kWh (1500 rpm, 100% load, 30 L/min, 0% EGR) NO_x = 6.8 g/kWh (1500 rpm, 100% load, 30 L/min, 30% EGR) NO_x = 4.56 g/kWh

HES: Hydrogen energy share.

All consulted authors, irrespective of engine size, demonstrated a consistent pattern of the effectiveness of EGR in reducing NO_x emissions. According to the work of Wu et al. [79] in a four-cylinder engine, at a 40% engine load, NO_x emissions were 900 ppm in diesel-fuel-only mode. Nevertheless, adding H_2 resulted in increased NO_x emissions (nearly up to 1400 ppm, with the maximum amount of injected H_2 8 L/min). At an EGR rate of 20% for this H_2 injection, NO_x emissions decreased to 283 ppm, resulting in a 68% reduction compared to the base case with diesel fuel. According to Vijayaragavan et al. [81], at full load in a single-cylinder engine, NO_x emissions were 5.09 g/kWh in diesel-fuel-only mode. However, the addition of H_2 increased NO_x emissions to 6.8 g/kWh. At an EGR rate of 30%, NO_x emissions dropped to 4.86 g/kWh, which means a 10% decline compared to the base case with diesel fuel. However, in certain scenarios, the use of EGR proved insufficient in minimizing emissions below the baseline, as demonstrated by Vimalananth et al. [66]. In that study, the initial emission level of 9.5 g/kWh without H_2 remained unaltered despite the application of the maximum EGR rate (10%).

The authors reported that raising the EGR rate lowers NO_x emissions due to dilutive and capacitive effects. Gnanamoorthi et al. [80] further explained that recirculated inert gases decreased O_2 levels and served as a heat sink. This resulted in a delayed combustion process until the expansion stroke. Subsequently, it caused lower combustion temperatures and, in turn, led to decreased NO_x formation. In addition to reducing NO_x emissions, EGR has been shown to decrease knocking through dilution effects [82,83]. As a result, EGR allowed for increased high-end torque without compromising system performance.

However, there are also drawbacks. Several authors have reported a reduction in engine performance due to the dilution effect. Regarding BTE, Chintala et al. [84] claimed that it decreased with EGR as a result of this effect. However, H_2 enrichment brought BTE back to levels similar to diesel fuel's base case. Nag et al. [54,83] reported that a slight enhancement in BTE was achieved for a 5% EGR rate at low loads. They attributed it to the recirculation of unburned fuel into the combustion chamber. However, at higher loads, the lack of unburnt fuel decreased the BTE, with this effect becoming more dominant as the load increased. Like H_2 enrichment of fresh air in the intake manifold, intake of recirculated gases displaced fresh air mass, reducing VE [54,81,82]. De Serio et al. [85] emphasized that dilutive and capacitive effects negatively impacted the combustion rate and resulted in reduced peak pressure values. Jafarmadar and Nemati [86] stated that a lack of oxygen caused a delay in ignition as EGR rates increased. Additionally, the mixture ignited with less intensity due to insufficient oxygen levels. Vimalananth et al. [66] reported a decrease in the heat release rate peak, delayed ignition, and a slight rise in the diffusion combustion

peak's area under the curve with EGR addition. They attributed it to an increase in the mixture-specific heat value, which lowered the overall combustion temperature and led to a higher CD.

The use of EGR with H_2 has proven to be an effective technique for reducing NO_x emissions. Nevertheless, relevant studies have shown that the dilution effect causes an increase in other pollutant emissions [50,54,66,79–82,87,88]. CO emissions increase with the EGR rate due to the O_2-deficient environment in the combustion chamber, thus lowering the in-cylinder temperature and reaction speed. This leads to a retardation of the oxidation reaction, resulting in higher production of CO [54]. The EGR rate also causes CO_2 emissions to increase because of additional CO_2 that is recirculated to the combustion chamber [54,79,87]. The decrease in oxygen results in a rise of HC and PM emissions, as restricted O_2 access leads to incomplete combustion, ultimately causing an increase in these emissions.

3.2. Water Injection

Another approach to mitigating high temperatures in the combustion chamber is through WI [89]. Inlet WI is considered the simpler option. There are several techniques documented in the literature, including multipoint WI in the intake pipes, near the inlet valves, or single-point injection upstream or downstream of the compressor [90]. The primary benefit of this method is its simple and easy integration into new or existing engines, which is similar to the intake manifold H_2 injection discussed in the previous section. In DWI, water is delivered directly into the combustion chamber using a dedicated injector with an electronic control that provides precise measurements of water volumes [91]. The integration of additional components to the existing engine system and redesigning the fuel supply system provide added complexity to this technique, unlike inlet WI. H_2 direct injection, which was discussed in the previous section, is one requirement for achieving this. In practice, the first two forms are more commonly used. Water diesel fuel emulsion (DWE) is an emulsion of water in standard diesel fuel that includes specific additives and surfactants for system stabilization [92]. Emulsion fuels have several deficiencies that hinder their widespread practical use. Additionally, the highly advanced and well-developed infrastructure required to implement this blend leads to excessive costs. Fuel's physical properties also change, which can significantly impact fuel injection system performance [91]. Consequently, practical application of emulsion fuels is still under investigation.

Numerous studies have investigated the impact of WI on CIEs. However, few have explored this technique in conjunction with H_2 in dual-fuel settings. Table 14 presents a comprehensive list of relevant studies that utilize different WI approaches, both experimentally and numerically. This table outlines the specific WI technique employed, the amount of H_2 supplied, and important findings.

Table 14. Results of the addition of H_2 and WI.

Ref.	H_2 Enrichment and Mixing Process Type of Test	Engine Specifications	Key Findings (NO_x=) Data Directly Reflected in the Document (NO_x≈) Approximately Measured Data in the Document Figures
[47]	0–2 kg/h Manifold inj. Type 3	Four cylinders Max. power: 63 kW at 4000 rpm Max. torque: 220 Nm at 1800 rpm Turbocharged	(1500 rpm, SOI = 10°,0.3 kg/h H_2, 0 kg/h H_2O) $NO_x \approx$ 850 ppm (1500 rpm, SOI = 10°, 0.3 kg/h H_2, 16 kg/h H_2O) $NO_x \approx$ 240 ppm (1500 rpm, SOI = 10°, 0.6 kg/h H_2, 16 kg/h H_2O) $NO_x \approx$ 750 ppm (1500 rpm, SOI = 10°, 0.6 kg/h H_2, 32 kg/h H_2O) $NO_x \approx$ 300 ppm (1500 rpm, SOI = 10°, 0.9 kg/h H_2, 32 kg/h H_2O) $NO_x \approx$ 810 ppm (1500 rpm, SOI = 10°, 0.9 kg/h H_2, 48 kg/h H_2O) $NO_x \approx$ 690 ppm
[93]	0–85% HES Manifold inj. Type 3	Four cylinders Max. power: 63 kW at 4000 rpm Max. torque: 220 Nm at 1800 rpm Turbocharged	(1500 rpm, SOI = 10°, 62% HES, 0 g/cycle H_2O) NO_x = 677 ppm (1500 rpm, SOI = 10°, 62% HES, 0.266 g/cycle H_2O) NO_x = 89 ppm (1500 rpm, SOI = 10°, 77% HES, 0.266 g/cycle H_2O) NO_x = 600 ppm (1500 rpm, SOI = 10°, 77% HES, 0.531 g/cycle H_2O) NO_x = 350 ppm (1500 rpm, SOI = 10°, 80% HES, 0.531 g/cycle H_2O) NO_x = 675 ppm (1500 rpm, SOI = 10°, 80% HES, 0.795 g/cycle H_2O) NO_x = 547 ppm

Table 14. *Cont.*

Ref.	H_2 Enrichment and Mixing Process Type of Test	Engine Specifications	Key Findings (NO_x=) Data Directly Reflected in the Document (NO_x≈) Approximately Measured Data in the Document Figures
[94]	0–1.6 H_2/diesel mass ratio Manifold inj. Type 3	Four cylinders Max. power: 63 kW at 4000 rpm Max. torque: 220 Nm at 1800 rpm Turbocharged	(2000 rpm, SOI = 10°, H_2/diesel ≈ 0.55, 0 kg/h H_2O) NO_x ≈ 900 ppm (2000 rpm, SOI = 10°, H_2/diesel ≈ 0.6, 16 kg/h H_2O) NO_x ≈ 350 ppm (2000 rpm, SOI = 10°, H_2/diesel ≈ 0.85, 16 kg/h H_2O) NO_x ≈ 620 ppm (2000 rpm, SOI = 10°, H_2/diesel ≈ 0.85, 32 kg/h H_2O) NO_x ≈ 250 ppm (2000 rpm, SOI = 10°, H_2/diesel ≈ 1.15, 32 kg/h H_2O) NO_x ≈ 450 ppm (2000 rpm, SOI = 10°, H_2/diesel ≈ 1.18, 48 kg/h H_2O) NO_x ≈ 380 ppm
[95]	20% HES Manifold inj. Type 1	Single cylinder Max. power: 7.4 kW at 1500 rpm Max. torque: No data Naturally aspirated	(1500 rpm, 100% load, 20% HES, 0 g/kWh H_2O) NO_x = 8.67 g/kWh (1500 rpm, 100% load, 20% HES, 130 g/kWh H_2O) NO_x = 8.24 g/kWh (1500 rpm, 100% load, 20% HES, 200 g/kWh H_2O) NO_x = 6.62 g/kWh (1500 rpm, 100% load, 20% HES, 270 g/kWh H_2O) NO_x = 5.47 g/kWh
[96]	0–36% HES Manifold inj. Type 1	Single cylinder Max. power: 7.4 kW at 1500 rpm Max. torque: No data Naturally aspirated	(1500 rpm, 100% load, 15% HES, 0 g/kWh H_2O) NO_x ≈ 9.3 g/kWh (1500 rpm, 100% load, 15% HES, 200 g/kWh H_2O) NO_x ≈ 6.2 g/kWh (1500 rpm, 100% load, 18% HES, 0 g/kWh H_2O) NO_x = 9.7 g/kWh (1500 rpm, 100% load, 18% HES, 200 g/kWh H_2O) NO_x = 6.6 g/kWh
[97]	0–66% HES Manifold inj. Type 1	Single cylinder Max. power: 7.4 kW at 1500 rpm Max. torque: No data Naturally aspirated	(1500 rpm, 100% load, 32% HES, 130 g/kWh H_2O) NO_x = 9.7 g/kWh (1500 rpm, 100% load, 32% HES, 270 g/kWh H_2O) NO_x = 6.5 g/kWh (1500 rpm, 100% load, 32% HES, 340 g/kWh H_2O) NO_x ≈ 6 g/kWh (1500 rpm, 100% load, 32% HES, 410 g/kWh H_2O) NO_x = 5.1 g/kWh
[98]	0–6.5% HES Manifold inj. Type 1	Single cylinder Max. power: 3.7 kW at 1500 rpm Max. torque: No data Naturally aspirated	(1500 rpm, 100% load, no H_2, 0% H_2O) NO = 289 ppm (1500 rpm, 100% load, 6.5% HES, 0% H_2O) NO = 465 ppm (1500 rpm, 100% load, 6.5% HES, 5% H_2O) NO ≈ 370 ppm
[99]	0–8% HES Manifold inj. Type 1	Single cylinder Max. power: 3.7 kW at 1500 rpm Max. torque: No data Naturally aspirated	Numerical study (1500 rpm, 100% load, 8% HES, 0% H_2O) P_{max} ≈ 12 MPa (1500 rpm, 100% load, 8% HES, 3% H_2O) P_{max} ≈ 11.8 MPa (1500 rpm, 100% load, 8% HES, 5% H_2O) P_{max} ≈ 11 MPa (1500 rpm, 100% load, 8% HES, 7% H_2O) P_{max} ≈ 10.5 MPa

HES: hydrogen energy share; P_{max}: maximum in-cylinder pressure.

All consulted authors, regardless of engine size or whether the test was numerical or experimental, indicated that WI is an effective strategy for reducing NO_x emissions. For instance, Serrano et al. [47] measured emissions of approximately 850 ppm by adding 0.3 kg/h of H_2 to a four-cylinder engine while keeping diesel fuel constant. By adding 16 kg/h of WI into the intake manifold, emissions were reduced to approximately 240 ppm, representing about a 70% reduction. By increasing the amount of hydrogen to 0.9 kg/h and using 48 kg/h of WI, emissions remained below the base case. However, more power was generated due to the increased amount of hydrogen. Emissions were approximately 690 ppm. In a single-cylinder engine at full load, Chintala and Subramanian [95] reported NO_x emissions of 8.67 g/kWh, with 20% HES. Emissions were reduced to 8.24, 6.62, and 5.47 g/kWh with 130, 200, and 270 g/kWh of water injection, respectively, resulting in a reduction of up to 37%.

The authors noted that WI reduced the combustion chamber temperature and, therefore, lowered NO_x emissions. Chintala and Subramanian [95] explained that WI also decreased O_2 concentration. Additionally, the introduction of water during suction stroke caused an increase in the mixture-specific heat, resulting in an overall decrease in temperature. Serrano et al. [94] demonstrated that WI resulted in thermal mechanism domination and minimum NO_x emissions. Moreover, they indicated that such emissions asymptotically decreased to a minimum. Thus, they suggested an upper limit of 48 kg/h of WI, beyond which there was no substantial effect on NO_x emissions.

Moreover, WI can extend the knock limit and increase HES in ICEs. Karthic et al. [98] conducted a study in which they achieved an HES increase from 6% to 8.5% using WI in a single-cylinder engine. Similarly, Chintala and Subramanian [95] observed that HES significantly increased with the quantity of WI. Specifically, HES increased from 20% (without WI) to 32%, 36%, and 39% with 130, 200, and 270 g/kWh of WI, respectively. However, BTE decreased with an increase in WI for a specific HES. Chintala and Subramanian [97] found that BTE decreased up to 3.3% when comparing cases with and without WI. They argued that WI resulted in a reduction of the in-cylinder temperature. In addition, Karthic et al. [98] utilized WI to increase HES, which was limited due to knocking problems. Increasing the

HES resulted in a higher BTE, thus reducing the impact of WI. Serrano et al. [100] argued that WI induced a cooling effect and an almost uniform water dispersion in the combustion chamber, thereby promoting increased VE. Similarly to EGR, replacing O_2 with water led to a delayed ignition and decreased HRR [94,95,98,101].

The use of WI with H_2 as an effective technique for reducing NO_x emissions has been demonstrated. However, according to the literature, the use of WI results in increased CO and HC emissions compared to the dual-fuel operation mode. This is due to the low temperature in the combustion chamber favoring NO_x reduction while reducing the oxidation of CO into CO_2 [95,98,102]. Chintala and Subramanian [95] argued that reducing the temperature decreased the flame speed. It led to cooling of the combustion chamber walls and incomplete combustion, thus increasing HC emissions. Taghavifar et al. [103] linked combustion chamber temperature reduction to an increase in PM emissions due to the reduced soot oxidation rate. This finding was previously found by Chintala and Subramanian [95]. They argued that the use of WI could harm the fuel–air mixing process, ultimately resulting in a higher degree of fuel heterogeneity.

3.3. Effect of Compression Rate Reduction

The last strategy examined in this study is the reduction of the CR. The CR refers to the proportion of cylinder volume and its headspace at the bottom of the piston stroke compared to the headspace volume at TDC [104]. Normally, the CIE CR ranges from 15:1 to 20:1. The CR directly affects combustion in two ways [105]. Firstly, it impacts the thermodynamic cycle. In fact, pressure and temperature at the end of compression are influenced by the CR. A higher CR increases both parameters. Combustion chamber geometry is also significantly affected by the CR, often resulting in a narrower aspect ratio with higher ratios. While some studies analyze the impact of the CR on CIEs in the context of WI, few have studied the influence of H_2. Moreover, most significant studies are those including biofuels. Table 15 displays relevant studies that integrate H_2 with various WI approaches, including experimental and numerical ones. This table presents the selected CR, supplied H_2, and essential findings.

Table 15. Results of the addition of H_2 and CR reduction.

Ref.	H_2 Enrichment and Mixing Process Type of Test	Engine Specifications	Key Findings (NO_x=) Data Directly Reflected in the Document (NO_x≈) Approximately Measured Data in the Document's Figures
[93]	0–85% HES Manifold inj. Type 3	Four cylinders Max. power: 63 kW at 4000 rpm Max. torque: 220 Nm at 1800 rpm Turbocharged	(1500 rpm, SOI = 10°, 62% HES, CR 17.5:1) NO_x = 903 ppm (1500 rpm, SOI = 10°, 62% HES, CR 16.3:1) NO_x = 744 ppm (1500 rpm, SOI = 10°, 62% HES, CR 15.5:1) NO_x = 677 ppm (1500 rpm, SOI = 10°, 62% HES, CR 14.5:1) NO_x = 653 ppm (1500 rpm, SOI = 10°, 62% HES, CR 13.5:1) NO_x = 510 ppm (2500 rpm, SOI = 10°, 70% HES, CR 17.5:1) NO_x = 868 ppm (2500 rpm, SOI = 10°, 70% HES, CR 16.3:1) NO_x = 469 ppm (2500 rpm, SOI = 10°, 70% HES, CR 15.5:1) NO_x = 302 ppm (2500 rpm, SOI = 10°, 70% HES, CR 14.5:1) NO_x = 273 ppm (2500 rpm, SOI = 10°, 70% HES, CR 13.5:1) NO_x = 208 ppm
[97]	0–66% HES Manifold inj. Type 1	Single cylinder Max. power: 7.4 kW at 1500 rpm Max. torque: No data Naturally aspirated	(1500 rpm, 100% load, no H2, CR 19.5:1, No WI) T_{cyl} = 1876 K (1500 rpm, 100% load, 19% HES, CR 19.5:1, WI) T_{cyl} = 1784 K (1500 rpm, 100% load, 19% HES, CR 16.5:1, WI) T_{cyl} = 1437 K (1500 rpm, 100% load, 19% HES, CR 15.4:1, WI) T_{cyl} = 1248 K
[99]	0–8% HES Manifold inj. Type 1	Single cylinder Max. power: 3.7 kW at 1500 rpm Max. torque: No data Naturally aspirated	Numerical study (1500 rpm, 100% load, 8% HES, CR 16.5:1) $P_{max} \approx$ 11.5 MPa (1500 rpm, 100% load, 8% HES, CR 16:1) $P_{max} \approx$ 11.2 MPa (1500 rpm, 100% load, 8% HES, CR 15.5:1) $P_{max} \approx$ 11 MPa (1500 rpm, 100% load, 8% HES, CR 15:1) $P_{max} \approx$ 10.5 MPa

Table 15. *Cont.*

Ref.	H_2 Enrichment and Mixing Process Type of Test	Engine Specifications	Key Findings (NO_x=) Data Directly Reflected in the Document (NO_x≈) Approximately Measured Data in the Document's Figures
[102]	0–63% HES Manifold inj. Type 1	Single cylinder Max. power: 7.4 kW at 1500 rpm Max. torque: No data Naturally aspirated	(1500 rpm, 100% load, no H_2, CR 19.5:1) NO_x = 6.8 g/kWh (1500 rpm, 100% load, 19% HES, CR 19.5:1) NO_x = 9.7 g/kWh (1500 rpm, 100% load, 19% HES, CR 16.5:1) NO_x = 5.5 g/kWh (1500 rpm, 100% load, 19% HES, CR 15.4:1) NO_x = 5 g/kWh (1500 rpm, 100% load, 58.8% HES, CR 16.5:1) NO_x ≈ 7 g/kWh (1500 rpm, 100% load, 62.6% HES, CR 15.4:1) NO_x ≈ 6.3 g/kWh
[106]	0.5 kg/h (H_2-enriched biogas) (HEB) Manifold inj. Type 2	Single cylinder Max. power: 3.5 kW at 1500 rpm Max. torque: No data Naturally aspirated	(1500 rpm, 0 bar, 0.5 kg/h HEB, CR 18:1) NO_x ≈ 10.2 g/kWh (1500 rpm, 0 bar, 0.5 kg/h HEB, CR 17:1) NO_x ≈ 9.2 g/kWh (1500 rpm, 0 bar, 0.5 kg/h HEB, CR 16:1) NO_x = 7.4 g/kWh (1500 rpm, 2.1 bar, 0.5 kg/h HEB, CR 18:1) NO_x ≈ 15 g/kWh (1500 rpm, 2.1 bar, 0.5 kg/h HEB, CR 17:1) NO_x ≈ 12 g/kWh (1500 rpm, 2.1 bar, 0.5 kg/h HEB, CR 16:1) NO_x ≈ 10.5 g/kWh (1500 rpm, 3.5 bar, 0.5 kg/h HEB, CR 18:1) NO_x = 16.5 g/kWh (1500 rpm, 3.5 bar, 0.5 kg/h HEB, CR 17:1) NO_x = 13.2 g/kWh (1500 rpm, 3.5 bar, 0.5 kg/h HEB, CR 16:1) NO_x = 12.6 g/kWh
[107]	0–55% HES Manifold inj. Type 1	Single cylinder Max. power: 7.4 kW at 1500 rpm Max. torque: No data Naturally aspirated	Numerical study (1500 rpm, 100% load, 10% HES, CR 19.5:1) NO_x ≈ 19.5 g/kWh (1500 rpm, 100% load, 10% HES, CR 16.5:1) NO_x ≈ 16.5 g/kWh (1500 rpm, 100% load, 10% HES, CR 14.5:1) NO_x ≈ 16 g/kWh (1500 rpm, 100% load, 30% HES, CR 19.5:1) NO_x ≈ 23 g/kWh (1500 rpm, 100% load, 30% HES, CR 16.5:1) NO_x ≈ 21.5 g/kWh (1500 rpm, 100% load, 30% HES, CR 14.5:1) NO_x ≈ 14.7 g/kWh (1500 rpm, 100% load, 55% HES, CR 19.5:1) NO_x ≈ 25.5 g/kWh (1500 rpm, 100% load, 55% HES, CR 16.5:1) NO_x ≈ 23.5 g/kWh (1500 rpm, 100% load, 55% HES, CR 14.5:1) NO_x ≈ 14.5 g/kWh

HES: hydrogen energy share; T_{cyl}: in-cylinder temperature; P_{max}: maximum in-cylinder pressure.

Regardless of engine size or testing methodology, all consulted authors indicated that reducing the CR is effective in decreasing NO_x emissions. Recently, authors of this review conducted a study on a four-cylinder car engine confirming this reduction [93]. At 1500 rpm and 62% HES, the results showed that for a standard engine CR (17.5:1), NO_x emissions were 903 ppm. Modifying the CR to 16.3:1, 15.5:1, 14.5:1, and 13.5:1 resulted in 744, 677, 653, and 510 ppm of NO_x emissions, respectively. A numerical study conducted by Sharma and Dhar [107] using a single-cylinder engine observed similar results to those of other authors during experimental developments. At 1500 rpm, full load, and 55%, the authors found NO_x emissions of 25.5, 23.5, and 14.5 g/kWh for CRs of 19.5:1, 16.5:1, and 14.5:1, respectively. In both studies, a maximum reduction of 43% in NO_x emissions was achieved. Similarly to WI, CR reduction resulted in a decrease in the maximum temperature within the combustion chamber, ultimately leading to a reduction in NO_x emissions [97,99,102,106–110].

Moreover, reducing the CR may improve knock limit extension while increasing HES. Chintala and Subramanian [102] found that decreasing the CR from 19.5:1 to 15.4:1 resulted in increased knock limits at 19%, 59%, and 63% HES, respectively. Similarly, Sharma and Dhar [107] reported an increase in knock limits from 20% to 45% HES as the CR decreased from 19.5:1 to 14.5:1. However, it should be noted that decreasing the CR may also lead to a decrease in BTE. Rosha et al. [106] found that BTE decreased from 36.1% to 34.4% and 32% for 16:1, 17:1, and 18:1 CRs, respectively. The authors argued that increasing the CR improved the BTE by enhancing the in-cylinder pressure and temperature. Additionally, in-cylinder temperature reduction caused a longer ID and CD.

In terms of emissions, the advantage of reducing NO_x emissions with CR reduction comes with some disadvantages. Lowering the combustion chamber temperature through CR reduction leads to slower and incomplete combustion, resulting in increased HC and soot emissions. As a consequence, the oxidation rate of CO into CO_2 is also reduced [106,107,109].

These methods for decreasing NO_x emissions may be compared and utilized in unison. In a study utilizing solely diesel fuel, Serrano et al. [100] compared the implementation of EGR with WI in the intake manifold. The authors stated that the use of WI was more effective than EGR at all engine speeds and under all engine loads. Additionally, Chintala and Subramanian [97] reported a reduction in NO_x when testing on a single-cylinder engine. They found that HES was limited to 18.8% in a conventional dual-fuel setup. However, it increased to 66.5% with the use of WI at 480 g/kWh. Moreover, it further increased to 79% with WI at 340 g/kWh (the selected optimum quantity) and a CR reduction from 19.5:1 to 16.5:1. Raju and Masimalai [99] conducted a numerical study on a single-cylinder engine, confirming previous studies on enhancing HES and reducing knocking and NO_x emissions. Additionally, authors of this review undertook a study on a four-cylinder commercial engine and found an almost linear relationship between the CR and NO_x [93]. As a result, decreasing the CR could promote NO_x reduction. Moreover, the use of WI further supports this reduction, as evidenced from Figure 3.

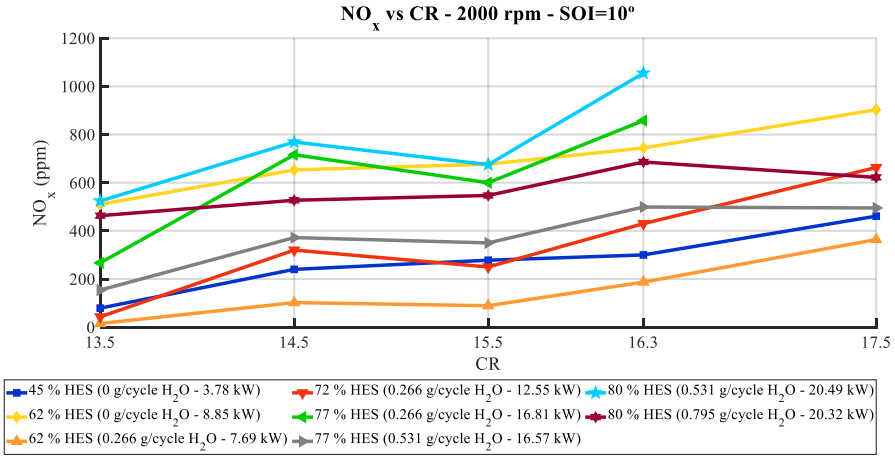

Figure 3. NO_x emissions versus compression ratio (CR) at 2000 rpm [93].

4. Conclusions

This review provides an overview of the utilization of H_2 and diesel fuel in dual-fuel mode for a sustainable energy solution for diesel engines. The subsequent conclusions are grounded in the outcomes obtained within the literature.

- The use of H_2 presents two obstacles that must be considered: knocking and backfiring. Too much H_2 increases the probability of knocking. Fortunately, backfiring can be remedied by proper injection of H_2 into the engine. Thus, choosing the optimal method for mixing air with H_2 is crucial.
- Among H_2 injection techniques (carburation, manifold, port, and direct injection), port injection provides superior outcomes for enhancing engine performance and reducing emissions. Nonetheless, direct injection shows potential as the superior option that may address the issue of backfiring. However, given the nonexistence of commercial H_2 injection solutions, it remains impractical at present.
- It is unclear how H_2 affects brake thermal efficiency (BTE) in terms of efficiency. While some studies have reported improved combustion and increased BTE with the addition of H_2, others have found incomplete combustion due to H_2. This issue, combined with higher thermal losses, may lead to lower BTE. Additionally, the introduction of H_2 into the combustion chamber tends to displace a significant amount of air, resulting in a decrease in volumetric efficiency (VE).
- The inclusion of H_2 in the combustion chamber, mixed with air, means that more energy is needed to increase the temperature of the mixture. This gas property justifies the increase in ignition delay (ID), as more time is required for the mixture's ignition to occur. Furthermore, hydrogen accelerates both premixed and diffusive phases,

resulting in a faster reaction compared to a reaction without hydrogen, which leads to a lower combustion duration (CD) and a higher maximum in-cylinder pressure.

- In terms of emissions, CO_2. CO, HC, and soot decrease with the addition of H_2. H_2 is a carbon-free fuel with a significant influence on the reduction of these emissions. In addition, it seems that this fuel's properties favor more complete combustion.
- The introduction of hydrogen in the chamber results in an increase in pressure rise rates and increased combustion temperatures. This tends to favor the Zeldovich mechanism for NO_x formation. Consequently, the addition of H_2 may need further NO_x reduction.
- Exhaust gas recirculation (EGR), water injection (WI), and compression ratio (CR) reduction are three effective NO_x reduction strategies. These approaches reduce combustion chamber temperature and, thus, NO_x emissions up to 70%. Furthermore, these techniques increase the knocking limit, which in turn increases the hydrogen energy share (HES).
- These techniques have a negative impact on both performance and emissions. They reduce BTE and increase ID and CD, thus leading to a decrease in the maximum in-cylinder pressure. Furthermore, combustion with these techniques promotes incomplete combustion. This, in turn, increases the emission levels of HC and soot, while reducing the oxidation rate of CO into CO_2. Despite this, the levels achieved may be lower than those observed during diesel fuel operation mode.

Author Contributions: Investigation, J.M.R.-V.; data curation, J.M.R.-V.; writing—original draft preparation, J.M.R.-V.; writing—review and editing, J.S., S.P., F.J.J.-E. and M.P.D.; supervision, J.S., S.P. and M.P.D. All authors have read and agreed to the published version of the manuscript.

Funding: We would like to express our gratitude to the Spanish Ministry of Science and Innovation for grants no. PID2019-105936RB-C21 and TED2021-130596B-C22 and Junta de Andalucía (Conserjería de Economía, Conocimiento, Empresas y Universidad) as part of item PY20 RE 010 within the "Incentivos a los agentes del sistema andaluz del conocimiento—Ayudas a la I+D+i, en el ámbito del Plan Andaluz de Investigación, Desarrollo e Innovación" (PAIDI 2020).

Data Availability Statement: Data are contained within the article.

Conflicts of Interest: The authors declare no conflicts of interest.

Nomenclature

BTE	Brake thermal efficiency	ICE	Internal combustion engine
CA	Crank angle	ID	Ignition delay
CD	Combustion duration	K	Opacity
CIE	Compression ignition engine	LHV	Lower heating value
CNG	Compressed natural gas	LL	Low load
CR	Compression rate	ML	Medium load
DWE	Water–diesel fuel emulsion	NG	Natural gas
DWI	Direct water injection	NTP	Normal temperature and pressure conditions
EGR	Exhaust gas recirculation	PM	Particulate matter
FCV	Fuel cell vehicle	SI	Spark ignition
GHG	Greenhouse gases	SOC	Start of combustion
HC	Hydrocarbons	SOI	Start of injection
HES	Hydrogen energy share	TDC	Top dead centre
HL	High load	VE	Volumetric efficiency
HRR	Heat release rate	WI	Water injection

References

1. European Commission. GHG Emissions of All World Countries 2023. Available online: https://edgar.jrc.ec.europa.eu/booklet/GHG_emissions_of_all_world_countries_booklet_2023report.pdf (accessed on 28 October 2023).
2. International Energy Agency. Assessing the Effects of Economic Recoveries on Global Energy Demand and CO_2 Emissions in 2021. Available online: https://www.iea.org/reports/global-energy-review-2021 (accessed on 28 October 2023).

3. Climate.gov. Climate Change: Atmospheric Carbon Dioxide. Available online: https://www.climate.gov/news-features/understanding-climate/climate-change-atmospheric-carbon-dioxide (accessed on 28 October 2023).
4. United Nations. United Nations, The Paris Agreement. Available online: https://www.un.org/en/climatechange/paris-agreement (accessed on 8 July 2022).
5. European Council. Climate Change: What the EU Is Doing. Available online: https://www.consilium.europa.eu/en/policies/climate-change/ (accessed on 8 July 2022).
6. European Commission. CO_2 Emission Performance Standards for Cars and Vans. Available online: https://climate.ec.europa.eu/eu-action/transport/road-transport-reducing-co2-emissions-vehicles/CO2-emission-performance-standards-cars-and-vans_en (accessed on 28 October 2023).
7. BP. BP Energy Outlook 2022. Available online: https://www.bp.com/content/dam/bp/business-sites/en/global/corporate/pdfs/energy-economics/energy-outlook/bp-energy-outlook-2022.pdf (accessed on 28 October 2023).
8. International Transport Forum. Executive Summary ITF Transport Outlook 2021. Available online: https://www.itf-oecd.org/sites/default/files/transport-outlook-executive-summary-2021-english.pdf (accessed on 8 July 2022).
9. McKinsey & Company. Global Energy Perspective 2022 Executive Summary. Available online: https://www.mckinsey.com/~/media/McKinsey/Industries/Oil%20and%20Gas/Our%20Insights/Global%20Energy%20Perspective%202022/Global-Energy-Perspective-2022-Executive-Summary.pdf (accessed on 8 July 2022).
10. Sandalci, T.; Karagöz, Y. Experimental Investigation of the Combustion Characteristics, Emissions and Performance of Hydrogen Port Fuel Injection in a Diesel Engine. *Int. J. Hydrogen Energy* **2014**, *39*, 18480–18489. [CrossRef]
11. Mohsin, R.; Majid, Z.A.; Shihnan, A.H.; Nasri, N.S.; Sharer, Z. Effect of Biodiesel Blends on Engine Performance and Exhaust Emission for Diesel Dual Fuel Engine. *Energy Convers. Manag.* **2014**, *88*, 821–828. [CrossRef]
12. Leiva-Candia, D.E.; García, I.L.; Lopez, I.; Serrano-Herrador, J.A.; Dorado, M.P. Descriptive and Inferential Statistics as an Exhaust Emission Comparative Tool between Different Engine Operating Conditions and Fuels. Application to Highly Oxidized Biodiesel Blended with Primary Alcohols. *Fuel* **2022**, *324*, 124453. [CrossRef]
13. Dorado, M.P. Raw Materials to Produce Low-Cost Biodiesel. In *Biofuels Refining and Performance*, 1st ed.; McGraw-Hill Education: New York, NY, USA, 2008.
14. Pinzi, S.; Leiva, D.; López-García, I.; Redel-Macías, M.D.; Dorado, M.P. Latest Trends in Feedstocks for Biodiesel Production. *Biofuels Bioprod. Biorefin.* **2014**, *8*, 126–143. [CrossRef]
15. International Energy Agency. Global Hydrogen Review 2021. Available online: https://www.iea.org/reports/global-hydrogen-review-2021 (accessed on 8 July 2022).
16. Muradov, N. Low to Near-Zero CO_2 Production of Hydrogen from Fossil Fuels: Status and Perspectives. *Int. J. Hydrogen Energy* **2017**, *42*, 14058–14088. [CrossRef]
17. Chi, J.; Yu, H. Water Electrolysis Based on Renewable Energy for Hydrogen Production. *Cuihua Xuebao/Chin. J. Catal.* **2018**, *39*, 390–394. [CrossRef]
18. Dimitriou, P.; Tsujimura, T. A Review of Hydrogen as a Compression Ignition Engine Fuel. *Int. J. Hydrogen Energy* **2017**, *42*, 24470–24486. [CrossRef]
19. Verhelst, S.; Wallner, T. Hydrogen-Fueled Internal Combustion Engines. *Prog. Energy Combust. Sci.* **2009**, *35*, 490–527. [CrossRef]
20. Rueda Vázquez, J.M.; Tejada Hernández, J.; Pinzi, S.; Dorado Pérez, M.; del, P. Bibliometric Study on Dual-Fuel Injection. In Proceedings of the 12 CNIT Proceedings Book, Madrid, Spain, 29 June 2022.
21. Kanth, S.; Debbarma, S. Comparative Performance Analysis of Diesel Engine Fuelled with Hydrogen Enriched Edible and Non-Edible Biodiesel. *Int. J. Hydrogen Energy* **2021**, *46*, 10478–10493. [CrossRef]
22. Pinto, G.M.; de Souza, T.A.Z.; da Costa, R.B.R.; Roque, L.F.A.; Frez, G.V.; Coronado, C.J.R. Combustion, Performance and Emission Analyses of a CI Engine Operating with Renewable Diesel Fuels (HVO/FARNESANE) under Dual-Fuel Mode through Hydrogen Port Injection. *Int. J. Hydrogen Energy* **2023**, *48*, 19713–19732. [CrossRef]
23. Rocha, H.M.Z.; Pereira, R.d.S.; Nogueira, M.F.M.; Belchior, C.R.P.; Tostes, M.E.; de, L. Experimental Investigation of Hydrogen Addition in the Intake Air of Compressed Ignition Engines Running on Biodiesel Blend. *Int. J. Hydrogen Energy* **2017**, *42*, 4530–4539. [CrossRef]
24. Tutak, W.; Jamrozik, A.; Grab-Rogaliński, K. Co-Combustion of Hydrogen with Diesel and Biodiesel (RME) in a Dual-Fuel Compression-Ignition Engine. *Energies* **2023**, *16*, 4892. [CrossRef]
25. Köse, H.; Ciniviz, M. An Experimental Investigation of Effect on Diesel Engine Performance and Exhaust Emissions of Addition at Dual Fuel Mode of Hydrogen. *Fuel Process. Technol.* **2013**, *114*, 26–34. [CrossRef]
26. Zheng, S.; He, Y.; Hu, B.; Zhu, J.; Zhou, B.; Lu, Q. Effects of Radiation Reabsorption on the Flame Speed and NO Emission of NH3/H2/Air Flames at Various Hydrogen Ratios. *Fuel* **2022**, *327*, 125176. [CrossRef]
27. Zheng, S.; He, Y.; Liu, H.; Yang, Y.; Han, W.; Lu, Q. Roles of Radiation Reabsorption on Flame Speed and NO Emission during Ammonia Combustion with Syngas Blending at Elevated Pressures. *Int. J. Hydrogen Energy* **2024**, *49*, 1336–1345. [CrossRef]
28. Najjar, Y.S.H. Hydrogen Safety: The Road toward Green Technology. *Int. J. Hydrogen Energy* **2013**, *38*, 10716–10728. [CrossRef]
29. Li, M.; Bai, Y.; Zhang, C.; Song, Y.; Jiang, S.; Grouset, D.; Zhang, M. Review on the Research of Hydrogen Storage System Fast Refueling in Fuel Cell Vehicle. *Int. J. Hydrogen Energy* **2019**, *44*, 10677–10693. [CrossRef]
30. Moradi, R.; Groth, K.M. Hydrogen Storage and Delivery: Review of the State of the Art Technologies and Risk and Reliability Analysis. *Int. J. Hydrogen Energy* **2019**, *44*, 12254–12269. [CrossRef]

31. Hwang, H.T.; Varma, A. Hydrogen Storage for Fuel Cell Vehicles. *Curr. Opin. Chem. Eng.* **2014**, *5*, 42–48. [CrossRef]
32. Stępień, Z. A Comprehensive Overview of Hydrogen-Fueled Internal Combustion Engines: Achievements and Future Challenges. *Energies* **2021**, *14*, 6504. [CrossRef]
33. Szwaja, S.; Grab-Rogalinski, K. Hydrogen Combustion in a Compression Ignition Diesel Engine. *Int. J. Hydrogen Energy* **2009**, *34*, 4413–4421. [CrossRef]
34. Hairuddin, A.A.; Yusaf, T.; Wandel, A.P. A Review of Hydrogen and Natural Gas Addition in Diesel HCCI Engines. *Renew. Sustain. Energy Rev.* **2014**, *32*, 739–761. [CrossRef]
35. Saravanan, N.; Nagarajan, G.; Narayanasamy, S. An Experimental Investigation on DI Diesel Engine with Hydrogen Fuel. *Renew. Energy* **2008**, *33*, 415–421. [CrossRef]
36. Castro, N.; Toledo, M.; Amador, G. An Experimental Investigation of the Performance and Emissions of a Hydrogen-Diesel Dual Fuel Compression Ignition Internal Combustion Engine. *Appl. Therm. Eng.* **2019**, *156*, 660–667. [CrossRef]
37. Bakar, R.A.; Widudo; Kadirgama, K.; Ramasamy, D.; Yusaf, T.; Kamarulzaman, M.K.; Sivaraos; Aslfattahi, N.; Samylingam, L.; Alwayzy, S.H. Experimental Analysis on the Performance, Combustion/Emission Characteristics of a DI Diesel Engine Using Hydrogen in Dual Fuel Mode. *Int. J. Hydrogen Energy* **2022**, *52*, 843–860. [CrossRef]
38. Das, L.M. Fuel induction techniques for a hydrogen operated engine. *Int. J. Hydrogen Energy* **1990**, *15*, 833–842. [CrossRef]
39. Chintala, V.; Subramanian, K.A. A Comprehensive Review on Utilization of Hydrogen in a Compression Ignition Engine under Dual Fuel Mode. *Renew. Sustain. Energy Rev.* **2017**, *70*, 472–491. [CrossRef]
40. de Troya Calatayud, J.J. Alternativa a los Combustibles Fósiles. Ph.D. Thesis, Utilización de Hidrógeno a Bordo de Buques, A Coruña, Spain, 2015.
41. Saravanan, N.; Nagarajan, G. Experimental Investigation in Optimizing the Hydrogen Fuel on a Hydrogen Diesel Dual-Fuel Engine. *Energy Fuels* **2009**, *23*, 2646–2657. [CrossRef]
42. Mohammadi, A.; Shioji, M.; Nakai, Y.; Ishikura, W.; Tabo, E. Performance and Combustion Characteristics of a Direct Injection SI Hydrogen Engine. *Int. J. Hydrogen Energy* **2007**, *32*, 296–304. [CrossRef]
43. Das, L.M. Hydrogen Engine: Research and Development (R&D) Programmes in Indian. Institute of Technology (IIT), Delhi. *Int. J. Hydrogen Energy* **2002**, *27*, 953–965.
44. Laforet, C.; Brown, B.; Rogak, S.; Munshi, S. Compression Ignition of Directly Injected Natural Gas with Entrained Diesel. *Int. J. Engine Res.-Int. J. Engine Res.* **2010**, *11*, 207–218. [CrossRef]
45. Liu, X.; Srna, A.; Yip, H.L.; Kook, S.; Chan, Q.N.; Hawkes, E.R. Performance and Emissions of Hydrogen-Diesel Dual Direct Injection (H2DDI) in a Single-Cylinder Compression-Ignition Engine. *Int. J. Hydrogen Energy* **2021**, *46*, 1302–1314. [CrossRef]
46. Yilmaz, I.T.; Demir, A.; Gumus, M. Effects of Hydrogen Enrichment on Combustion Characteristics of a CI Engine. *Int. J. Hydrogen Energy* **2017**, *42*, 10536–10546. [CrossRef]
47. Serrano, J.; Jiménez-Espadafor, F.J.; López, A. Analysis of the Effect of the Hydrogen as Main Fuel on the Performance of a Modified Compression Ignition Engine with Water Injection. *Energy* **2019**, *173*, 911–925. [CrossRef]
48. Egúsquiza, J.C.C.; Braga, S.L.; Braga, C.V.M. *Experimental Investigation of a Diesel Engine Operating on Natural Gas/Diesel Dual-Fuel Mode*; SAE Technical Paper; SAE International: Warrendale, PA, USA, 2011; p. 12. [CrossRef]
49. Barrios, C.C.; Domínguez-Sáez, A.; Hormigo, D. Influence of Hydrogen Addition on Combustion Characteristics and Particle Number and Size Distribution Emissions of a TDI Diesel Engine. *Fuel* **2017**, *199*, 162–168. [CrossRef]
50. Hoang, A.T.; Pham, V.V. A Study on a Solution to Reduce Emissions by Using Hydrogen as an Alternative Fuel for a Diesel Engine Integrated Exhaust Gas Recirculation. In Proceedings of the AIP Conference Proceedings, Namakkal, India, 4 May 2020; American Institute of Physics Inc.: College Park, MD, USA, 2020; Volume 2235.
51. Yilmaz, I.T.; Gumus, M. Effects of Hydrogen Addition to the Intake Air on Performance and Emissions of Common Rail Diesel Engine. *Energy* **2018**, *142*, 1104–1113. [CrossRef]
52. Wu, Y.; Devi, P.B.; Anbarasu, A.; Sołowski, G.; Chanh, H.C.; Chi, N.T.L.; Nasif, O.; Alharbi, S.A.; Xia, C. Estimation of the Engine Performance and Emission Characteristics of Hydrogen Feed Vehicles with Modified Injection Fuel System. *Fuel* **2022**, *329*, 125339. [CrossRef]
53. Das, S.; Kanth, S.; Das, B.; Debbarma, S. Experimental Evaluation of Hydrogen Enrichment in a Dual-Fueled CRDI Diesel Engine. *Int. J. Hydrogen Energy* **2022**, *47*, 11039–11051. [CrossRef]
54. Nag, S.; Sharma, P.; Gupta, A.; Dhar, A. Experimental Study of Engine Performance and Emissions for Hydrogen Diesel Dual Fuel Engine with Exhaust Gas Recirculation. *Int. J. Hydrogen Energy* **2019**, *44*, 12163–12175. [CrossRef]
55. Sharma, P.; Dhar, A. Effect of Hydrogen Supplementation on Engine Performance and Emissions. *Int. J. Hydrogen Energy* **2018**, *43*, 7570–7580. [CrossRef]
56. Subramanian, B.; Thangavel, V. Experimental Investigations on Performance, Emission and Combustion Characteristics of Diesel-Hydrogen and Diesel-HHO Gas in a Dual Fuel CI Engine. *Int. J. Hydrogen Energy* **2020**, *45*, 25479–25492. [CrossRef]
57. Owston, R.; Magi, V.; Abraham, J. *Wall Interactions of Hydrogen Flames Compared with Hydrocarbon Flames*; SAE International: Warrendale, PA, USA, 2007; Volume 116.
58. Bennett, S. *Modern Diesel Technology: Diesel Engines*; Cengage Learning: Belmont, CA, USA, 2014; ISBN 9781305177987.
59. Lakshminarayanan, P.A.; Aghav, Y. V Ignition Delay in a Diesel Engine. In *Modelling Diesel Combustion*; Lakshminarayanan, P.A., Aghav, Y.V., Eds.; Springer: Dordrecht, The Netherlands, 2010; pp. 59–78, ISBN 978-90-481-3885-2.

60. Jabbr, A.I.; Koylu, U.O. Influence of Operating Parameters on Performance and Emissions for a Compression-Ignition Engine Fueled by Hydrogen/Diesel Mixtures. *Int. J. Hydrogen Energy* **2019**, *44*, 13964–13973. [CrossRef]
61. Aldhaidhawi, M.; Chiriac, R.; Badescu, V. Ignition Delay, Combustion and Emission Characteristics of Diesel Engine Fueled with Rapeseed Biodiesel—A Literature Review. *Renew. Sustain. Energy Rev.* **2017**, *73*, 178–186. [CrossRef]
62. Dhole, A.E.; Yarasu, R.B.; Lata, D.B. Investigations on the Combustion Duration and Ignition Delay Period of a Dual Fuel Diesel Engine with Hydrogen and Producer Gas as Secondary Fuels. *Appl. Therm. Eng.* **2016**, *107*, 524–532. [CrossRef]
63. Lata, D.B.; Bhushan Kumar, C. Experimental Analysis of Ignition Delay in Dual-Fuel Diesel Engine with Secondary Fuel. *Int. J. Res. Anal. Rev. (IJRAR)* **2018**, *251*, 279–285.
64. Juknelevicius, R.; Szwaja, S.; Pyrc, M.; Gruca, M. Influence of Hydrogen Co-Combustion with Diesel Fuel on Performance, Smoke and Combustion Phases in the Compression Ignition Engine. *Int. J. Hydrogen Energy* **2019**, *44*, 19026–19034. [CrossRef]
65. Cernat, A.; Pana, C.; Negurescu, N.; Lazaroiu, G.; Nutu, C.; Fuiorescu, D. Hydrogen—An Alternative Fuel for Automotive Diesel Engines Used in Transportation. *Sustainability* **2020**, *12*, 9321. [CrossRef]
66. Vimalananth, V.T.; Panithasan, M.S.; Venkadesan, G. Investigating the Effects of Injection and Induction Modes of Hydrogen Addition in a CRDI Pilot Diesel-Fuel Engine with Exhaust Gas Recirculation. *Int. J. Hydrogen Energy* **2022**, *47*, 22559–22573. [CrossRef]
67. Kozak, M.; Merkisz, J. Oxygenated Diesel Fuels and Their Effect on PM Emissions. *Appl. Sci.* **2022**, *12*, 7709. [CrossRef]
68. Payri González, F.; Desantes Fernández, J.M. *Motores de Combustión Interna Alternativos*; Reverté: Barcelona, Spain, 2011; ISBN 9788429148022.
69. Ghazal, O.H. Performance and Combustion Characteristic of CI Engine Fueled with Hydrogen Enriched Diesel. *Int. J. Hydrogen Energy* **2013**, *38*, 15469–15476. [CrossRef]
70. Edward, K. Chapter 18—Air Pollution. In *Environmental Pollution and Control*, 4th ed.; Peirce, J.J., Weiner, R.F., Vesilind, P.A., Eds.; Butterworth-Heinemann: Woburn, MA, USA, 1998; pp. 245–269, ISBN 978-0-7506-9899-3.
71. Mullinger, P.; Jenkins, B. Chapter 2—The Combustion Process. In *Industrial and Process Furnaces*, 2nd ed.; Mullinger, P., Jenkins, B., Eds.; Butterworth-Heinemann: Oxford, UK, 2013; pp. 31–65, ISBN 978-0-08-099377-5.
72. Saravanan, N.; Nagarajan, G. Performance and Emission Studies on Port Injection of Hydrogen with Varied Flow Rates with Diesel as an Ignition Source. *Appl. Energy* **2010**, *87*, 2218–2229. [CrossRef]
73. Bosch, H.; Janssen, F. Catalytic Reduction of Nitrogen Oxides—A Review on the Fundamentals and Technology. *Catal. Today* **1988**, *2*, 4.
74. Hoekman, S.K.; Robbins, C. Review of the Effects of Biodiesel on NOx Emissions. *Fuel Process. Technol.* **2012**, *96*, 237–249. [CrossRef]
75. Warnatz, J.; Maas, U.; Dibble, R. *Combustion: Physical and Chemical Fundamentals, Modeling and Simulation, Experiments, Pollutant Formation*; Springer: Berlin/Heidelberg, Germany, 2006; ISBN 978-3-540-25992-3.
76. Gomes Antunes, J.M.; Mikalsen, R.; Roskilly, A.P. An Investigation of Hydrogen-Fuelled HCCI Engine Performance and Operation. *Int. J. Hydrogen Energy* **2008**, *33*, 5823–5828. [CrossRef]
77. Heywood, J.B. *Internal Combustion Engine Fundamentals*, 2nd ed.; McGraw-Hill Education: New York, NY, USA, 2018; ISBN 9781260116106.
78. Talibi, M.; Hellier, P.; Ladommatos, N. The Effect of Varying EGR and Intake Air Boost on Hydrogen-Diesel Co-Combustion in CI Engines. *Int. J. Hydrogen Energy* **2017**, *42*, 6369–6383. [CrossRef]
79. Wu, H.W.; Hsu, T.Z.; Lai, W.H. Dual Fuel Turbocharged Engine Operated with Exhaust Gas Recirculation. *J. Mech.* **2018**, *34*, 21–27. [CrossRef]
80. Gnanamoorthi, V.; Vimalananth, V.T.; Murugan, M. Effect of EGR on ci engine fuelled with diesel and hydrogen. *Int. Res. J. Eng. Technol.* **2018**, *5*, 1642–1648.
81. Vijayaragavan, M.; Subramanian, B.; Sudhakar, S.; Natrayan, L. Effect of Induction on Exhaust Gas Recirculation and Hydrogen Gas in Compression Ignition Engine with Simarouba Oil in Dual Fuel Mode. *Int. J. Hydrogen Energy* **2022**, *47*, 37635–37647. [CrossRef]
82. Chaichan, M.T. Performance and Emission Characteristics of CIE Using Hydrogen, Biodiesel, and Massive EGR. *Int. J. Hydrogen Energy* **2018**, *43*, 5415–5435. [CrossRef]
83. Nag, S.; Dhar, A.; Gupta, A. Hydrogen-Diesel Co-Combustion Characteristics, Vibro-Acoustics and Unregulated Emissions in EGR Assisted Dual Fuel Engine. *Fuel* **2022**, *307*, 121925. [CrossRef]
84. Chintala, V.; Benaerjee, D.; Ghodke, P.K.; Porpatham, E. Hydrogen Rich Exhaust Gas Recirculation (H2EGR) for Performance Improvement and Emissions Reduction of a Compression Ignition Engine. *Int. J. Hydrogen Energy* **2019**, *44*, 18545–18558. [CrossRef]
85. De Serio, D.; de Oliveira, A.; Sodré, J.R. Effects of EGR Rate on Performance and Emissions of a Diesel Power Generator Fueled by B7. *J. Braz. Soc. Mech. Sci. Eng.* **2017**, *39*, 1919–1927. [CrossRef]
86. Jafarmadar, S.; Nemati, P. Analysis of Exhaust Gas Recirculation (EGR) Effects on Exergy Terms in an Engine Operating with Diesel Oil and Hydrogen. *Energy* **2017**, *126*, 746–755. [CrossRef]
87. Dahake, M.R.; Malkhede, D.N. Experimental Investigation of Performance and Emissions of CRDI Diesel Engine in Dual Fuel Mode by Hydrogen Induction and Diesel Injection Coupled with Exhaust Gas Recirculation. *Proc. Mater. Today* **2021**, *46*, 2814–2819. [CrossRef]

88. Yaliwal, V.S.; Banapurmath, N.R.; Soudagar, M.E.M.; Afzal, A.; Ahmadi, P. Effect of Manifold and Port Injection of Hydrogen and Exhaust Gas Recirculation (EGR) in Dairy Scum Biodiesel—Low Energy Content Gas-Fueled CI Engine Operated on Dual Fuel Mode. *Int. J. Hydrogen Energy* **2022**, *47*, 6873–6897. [CrossRef]
89. Tauzia, X.; Maiboom, A.; Shah, S.R. Experimental Study of Inlet Manifold Water Injection on Combustion and Emissions of an Automotive Direct Injection Diesel Engine. *Energy* **2010**, *35*, 3628–3639. [CrossRef]
90. Sahin, Z.; Tuti, M.; Durgun, O. Experimental Investigation of the Effects of Water Adding to the Intake Air on the Engine Performance and Exhaust Emissions in a Di Automotive Diesel Engine. *Fuel* **2014**, *115*, 884–895. [CrossRef]
91. Tesfa, B.; Mishra, R.; Gu, F.; Ball, A.D. Water Injection Effects on the Performance and Emission Characteristics of a CI Engine Operating with Biodiesel. *Renew. Energy* **2012**, *37*, 333–344. [CrossRef]
92. Lif, A.; Holmberg, K. Water-in-Diesel Emulsions and Related Systems. *Adv. Colloid Interface Sci.* **2006**, *123–126*, 231–239. [CrossRef]
93. Rueda-Vázquez, J.M.; Serrano, J.; Jiménez-Espadafor, F.J.; Dorado, M.P. Experimental Analysis of the Effect of Hydrogen as the Main Fuel on the Performance and Emissions of a Modified Compression Ignition Engine with Water Injection and Compression Ratio Reduction. *Appl. Therm. Eng.* **2024**, *238*, 121933. [CrossRef]
94. Serrano, J.; Jiménez-Espadafor, F.J.; López, A. Analysis of the Effect of Different Hydrogen/Diesel Ratios on the Performance and Emissions of a Modified Compression Ignition Engine under Dual-Fuel Mode with Water Injection. Hydrogen-Diesel Dual-Fuel Mode. *Energy* **2019**, *172*, 702–711. [CrossRef]
95. Chintala, V.; Subramanian, K.A. Hydrogen Energy Share Improvement along with NOx (Oxides of Nitrogen) Emission Reduction in a Hydrogen Dual-Fuel Compression Ignition Engine Using Water Injection. *Energy Convers. Manag.* **2014**, *83*, 249–259. [CrossRef]
96. Chintala, V.; Subramanian, K.A. An Effort to Enhance Hydrogen Energy Share in a Compression Ignition Engine under Dual-Fuel Mode Using Low Temperature Combustion Strategies. *Appl. Energy* **2015**, *146*, 174–183. [CrossRef]
97. Chintala, V.; Subramanian, K.A. Experimental Investigation of Hydrogen Energy Share Improvement in a Compression Ignition Engine Using Water Injection and Compression Ratio Reduction. *Energy Convers. Manag.* **2016**, *108*, 106–119. [CrossRef]
98. Karthic, S.V.; Senthil Kumar, M.; Pradeep, P.; Vinoth Kumar, S. Assessment of Hydrogen-Based Dual Fuel Engine on Extending Knock Limiting Combustion. *Fuel* **2020**, *260*, 116342. [CrossRef]
99. Raju, P.; Masimalai, S. Numerical Study on a Diesel–Hydrogen Dual-Fuel Engine with Water Injection and Variable Compression Ratio. *Energy Technol.* **2022**, *10*, 2100626. [CrossRef]
100. Serrano, J.; Jiménez-Espadafor, F.J.; Lora, A.; Modesto-López, L.; Gañán-Calvo, A.; López-Serrano, J. Experimental Analysis of NOx Reduction through Water Addition and Comparison with Exhaust Gas Recycling. *Energy* **2019**, *168*, 737–752. [CrossRef]
101. Ghazal, O.H. Combustion Analysis of Hydrogen-Diesel Dual Fuel Engine with Water Injection Technique. *Case Stud. Therm. Eng.* **2019**, *13*, 100380. [CrossRef]
102. Chintala, V.; Subramanian, K.A. Experimental Investigations on Effect of Different Compression Ratios on Enhancement of Maximum Hydrogen Energy Share in a Compression Ignition Engine under Dual-Fuel Mode. *Energy* **2015**, *87*, 448–462. [CrossRef]
103. Taghavifar, H.; Anvari, S.; Parvishi, A. Benchmarking of Water Injection in a Hydrogen-Fueled Diesel Engine to Reduce Emissions. *Int. J. Hydrogen Energy* **2017**, *42*, 11962–11975. [CrossRef]
104. Dell, R.M.; Moseley, P.T.; Rand, D.A.J. Chapter 4—Development of Road Vehicles with Internal-Combustion Engines. In *Towards Sustainable Road Transport*; Dell, R.M., Moseley, P.T., Rand, D.A.J., Eds.; Academic Press: Boston, MA, USA, 2014; pp. 109–156, ISBN 978-0-12-404616-0.
105. Winterbone, D.E.; Turan, A. Chapter 16—Reciprocating Internal Combustion Engines. In *Advanced Thermodynamics for Engineers*, 2nd ed.; Winterbone, D.E., Turan, A., Eds.; Butterworth-Heinemann: Boston, MA, USA, 2015; pp. 345–379, ISBN 978-0-444-63373-6.
106. Rosha, P.; Kumar, S.; Senthil Kumar, P.; Kowthaman, C.N.; Kumar Mohapatra, S.; Dhir, A. Impact of Compression Ratio on Combustion Behavior of Hydrogen Enriched Biogas-Diesel Operated CI Engine. *Fuel* **2022**, *310*, 122321. [CrossRef]
107. Sharma, P.; Dhar, A. Compression Ratio Influence on Combustion and Emissions Characteristic of Hydrogen Diesel Dual Fuel CI Engine: Numerical Study. *Fuel* **2018**, *222*, 852–858. [CrossRef]
108. Sanli, A.; Yılmaz, I.T.; Gümüş, M. Assessment of Combustion and Exhaust Emissions in a Common-Rail Diesel Engine Fueled with Methane and Hydrogen/Methane Mixtures under Different Compression Ratio. *Int. J. Hydrogen Energy* **2020**, *45*, 3263–3283. [CrossRef]
109. Masood, M.; Mehdi, S.N.; Reddy, P.R. Experimental Investigations on a Hydrogen-Diesel Dual Fuel Engine at Different Compression Ratios. *J. Eng. Gas. Turbine Power* **2007**, *129*, 572–578. [CrossRef]
110. Yilmaz, I.T. The Effect of Hydrogen on the Thermal Efficiency and Combustion Process of the Low Compression Ratio CI Engine. *Appl. Therm. Eng.* **2021**, *197*, 117381. [CrossRef]